



HAL
open science

Averaged Steklov Eigenvalues, Inside Outside Duality and Application to Inverse Scattering

Lorenzo Audibert, Housseem Haddar, Fabien Pourre

► **To cite this version:**

Lorenzo Audibert, Housseem Haddar, Fabien Pourre. Averaged Steklov Eigenvalues, Inside Outside Duality and Application to Inverse Scattering. 2025. hal-04911173

HAL Id: hal-04911173

<https://inria.hal.science/hal-04911173v1>

Preprint submitted on 24 Jan 2025

HAL is a multi-disciplinary open access archive for the deposit and dissemination of scientific research documents, whether they are published or not. The documents may come from teaching and research institutions in France or abroad, or from public or private research centers.

L'archive ouverte pluridisciplinaire **HAL**, est destinée au dépôt et à la diffusion de documents scientifiques de niveau recherche, publiés ou non, émanant des établissements d'enseignement et de recherche français ou étrangers, des laboratoires publics ou privés.



Distributed under a Creative Commons Attribution 4.0 International License

Averaged Steklov Eigenvalues, Inside Outside Duality and Application to Inverse Scattering

Lorenzo Audibert*, Housseem Haddar†, and Fabien Poudre†

Abstract. We introduce a new family of artificial backgrounds corresponding to averaged impedance boundary conditions formulated in an abstract framework. These backgrounds are used to define a finite number of averaged Steklov eigenvalues, which are associated with inverse scattering problems from inhomogeneous media. We prove that these special eigenvalues can be determined from full-aperture, fixed-frequency far-fields using the inside-outside duality method. We then show and numerically demonstrate how this method can be used to reconstruct averaged values of the refractive index.

Key words. Averaged Steklov Eigenvalue, Inverse Scattering, Inside Outside duality, Artificial Background.

AMS subject classifications. 35J05, 35R30, 65M32, 93B60

1. Introduction. This work is motivated by the study of fixed-frequency inverse scattering problems using multistatic data. Specifically, our goal is to develop new inversion algorithms that avoid the use of forward solvers, in the sense of linear sampling methods [21, 11], and that can be applied to the imaging of complex media. This new class of algorithms uses spectral signatures to infer either an indicator function for defects or averaged values of material properties [4, 8, 7].

An example of spectral signatures is the so-called transmission eigenvalues [11, 15]. Their connection with the material properties of the scatterer [11] and the possibility of recovering them from far-field data [10, 6] have led to an imaging method in [4] that provides a quantitative indicator of crack density. The latter inspired the development of analogous fixed-frequency imaging algorithms. In these algorithms, transmission eigenvalues are replaced by artificial spectral parameters associated with artificial backgrounds [8, 7].

The use of artificial backgrounds for the construction of spectral signatures or for the design of imaging algorithms has been explored in various ways in the literature [14, 13, 2, 18, 12, 1]. The objective of this paper is to focus on the concept of averaged Steklov eigenvalues as introduced in [8, 7]. The main advantage is that the spectrum is very simple, since it contains only one non-trivial eigenvalue. This has significant implications for the robustness and accuracy of the associated imaging algorithm.

The novel contributions of this paper are threefold. Firstly, we present a more general definition of averaged Steklov eigenvalues by formulating the underlying impedance boundary condition with an abstract boundary operator of finite rank $M \geq 1$. This results in spectral problems with M nonzero eigenvalues (the parameter M can be chosen arbitrarily). In fact, the abstract model includes the explicit models used in [7] with $M = 1$. Further examples of such operators with $M > 1$ are provided in the numerical section.

The second new contribution is the analysis of the so-called Inside-Outside Duality Method (IODM) [17, 22] which is used to retrieve these spectral parameters. This is in contrast to

*Departement PRISME, EDF R&D, 6 quai Watier BP 49 Chatou, 78401 Cedex, France

†Inria, UMA, ENSTA Paris, Institut Polytechnique de Paris, 91120 Palaiseau, France

39 the work in [4, 7], where a different method is used based on the generalized linear sampling
 40 method. The IODM was initially proposed for Dirichlet eigenvalues [22]. It has since been
 41 extended to the identification of transmission eigenvalues in [22, 23] under some restrictive
 42 assumptions on the material parameters. For a special design of the background parameters
 43 in [19, 3] these restrictions were removed. In the present work we will show that the simple
 44 structure of the impedance boundary conditions allows a necessary and sufficient condition
 45 to characterize the spectral parameters in terms of the phase of the eigenvalues of a modified
 46 far-field operator.

47 Since there are only a few spectral parameters, the IODM allows a simple numerical
 48 implementation (compared to the cases in [23, 19]) and provides a faster and more reliable
 49 alternative to the method in [6]. This is the core of our third novel contribution. The
 50 efficiency of this method is demonstrated by revisiting the imaging algorithm in [7], which
 51 uses the IODM to identify the spectral parameter and reconstruct the averaged values of the
 52 refractive index.

53 The paper is organized as follows. Section 2 is devoted to the definition of the artificial
 54 background with an abstract formulation of the associated impedance boundary conditions.
 55 We then define the associated averaged Steklov eigenvalues (called \mathcal{B} -eigenvalues). In Section
 56 3 we introduce the inverse problem for inhomogeneous media and define a modified far field
 57 operator relative to the artificial background. A key factorization of this far field operator
 58 is then given. Section 4 contains the main theoretical result of this work, which is the char-
 59 acterization of the \mathcal{B} -eigenvalues using the IODM. In Section 5 we propose some validating
 60 numerical tests against analytical expressions obtained for circular domains. We then propose
 61 an algorithm implementing the IODM that can be used in the imaging algorithm proposed
 62 in [7]. We conclude with some validating numerical examples where we reconstruct the mean
 63 value of refractive index of the probed medium from noisy far field data. Some technical
 64 results are given in an appendix.

65 **2. Averaged Steklov Eigenvalues.** Let D be a bounded domain in \mathbb{R}^m , $m = 2, 3$ with
 66 piecewise smooth boundary ∂D and connected complement. We denote by ν the outward
 67 normal field on ∂D . We shall consider the following scattering problem, with inhomogeneity
 68 supported in D . This inhomogeneity is characterized by a real refractive index $n \in L^\infty(\mathbb{R}^m)$
 69 such that $n > 0$ and $n = 1$ in $\mathbb{R}^m \setminus \overline{D}$. For $k > 0$ being the wavenumber, the total field
 70 $u \in H_{loc}^1(\mathbb{R}^m)$ associated with some given incident field u^i satisfies the following equations

$$71 \quad (2.1) \quad \begin{cases} \Delta u + k^2 n u = 0 \text{ in } \mathbb{R}^m, \\ u = u^s + u^i, \\ \lim_{R \rightarrow +\infty} \int_{|x|=R} \left| \frac{\partial u^s}{\partial r} - i k u^s \right|^2 ds = 0, \end{cases}$$

72 where the incident field is assumed to satisfy the Helmholtz equation in \mathbb{R}^m . The motivation
 73 of the following developments is to infer some macroscopic properties of the refractive index
 74 n from measurements of the far fields associated with incident plane waves. To do so, we
 75 shall further develop the approach proposed in [4] by exploiting the notion of modified trans-
 76 mission eigenvalues relative to some artificial background media. In the context here, these
 77 eigenvalues correspond with Steklov-like eigenvalues since we shall use a background media
 78 that correspond with a generalization of the one introduced in [8, 7]. More precisely, we

79 shall consider the following model for the background media: the total field for the artificial
 80 background media, denoted by $u_b \in H_{loc}^1(\mathbb{R}^m \setminus D_b)$ satisfies the following equations

$$81 \quad (2.2) \quad \begin{cases} \Delta u_b + k^2 u_b = 0 \text{ in } \mathbb{R}^m \setminus D_b, \\ \mu u_b + \mathcal{B}(\partial_\nu u_b) = 0 \text{ on } \partial D_b \\ u_b = u_b^s + u^i \\ \lim_{R \rightarrow +\infty} \int_{|x|=R} \left| \frac{\partial u_b^s}{\partial r} - i k u_b^s \right|^2 ds = 0, \end{cases}$$

82 for some incident field u^i and for some parameter $\mu \in \mathbb{R}$. The domain $D_b \subset \mathbb{R}^m$ is supposed
 83 to be regular, bounded and simply connected. For simplicity, we assume that $D \subset D_b$. This
 84 assumption can be weakened as we shall later explain in Remark 4.10 (Section 4).

85 The operator $\mathcal{B} : H^{-\frac{1}{2}}(\partial D_b) \rightarrow H^{\frac{1}{2}}(\partial D_b)$ in the boundary condition in (2.2) is supposed
 86 to be of finite rank. More specifically, in all of the following, we assume that the following
 87 hypothesis holds true for the operator \mathcal{B} .

88 **Assumption 2.1.** *There exists a family of M vectors $\{e_1, \dots, e_M\} \subset H^{\frac{1}{2}}(\partial D_b)$ which are*
 89 *orthonormal with respect to the $L^2(\partial D_b)$ scalar product and a positive real constant κ such*
 90 *that:*

$$91 \quad (2.3) \quad \mathcal{B}(\psi) = \kappa \sum_{i=1}^M \langle \psi, e_i \rangle_{H^{-\frac{1}{2}}(\partial D_b), H^{\frac{1}{2}}(\partial D_b)} e_i, \quad \forall \psi \in H^{-\frac{1}{2}}(\partial D_b).$$

92

93 This assumption implies in particular that the operator \mathcal{B} satisfies:

$$94 \quad (2.4) \quad \kappa(\mathcal{B}\psi, \mathcal{B}\phi)_{L^2(\partial D_b)} = \langle \psi, \mathcal{B}\phi \rangle_{H^{-\frac{1}{2}}(\partial D_b), H^{\frac{1}{2}}(\partial D_b)},$$

95 for all $\psi, \phi \in H^{-\frac{1}{2}}(\partial D_b)$. In fact, this property (2.4) is also a sufficient condition for the
 96 operator \mathcal{B} to be of the form (2.3) (see A).

97 Using (2.4), one can prove, by standard variational techniques, that the direct problem
 98 (2.2) is well posed. The details are also given in A.

99 **Definition 2.2.** *A non zero real μ is called a \mathcal{B} -averaged Steklov eigenvalue (in short*
 100 *\mathcal{B} -eigenvalue) if there exists $w_0 \in H^1(D_b)$ non trivial solution of*

$$101 \quad (2.5) \quad \begin{cases} \Delta w_0 + k^2 n w_0 = 0 \text{ in } D_b, \\ \mu w_0 + \mathcal{B}(\partial_\nu w_0) = 0 \text{ on } \partial D_b. \end{cases}$$

102 Let us assume that k^2 is not a Dirichlet eigenvalue of the following problem:

$$103 \quad (2.6) \quad \begin{cases} v \in H^1(D_b), \\ \Delta v + k^2 n v = 0 \text{ in } D_b, \quad v = 0 \text{ on } \partial D_b. \end{cases}$$

104 Then one can construct M functions $w_i \in H^1(D_b)$, $i = 1, \dots, M$ solution of:

$$105 \quad (2.7) \quad \begin{cases} \Delta w_i + k^2 n w_i = 0 \text{ in } D_b, \\ w_i = e_i \text{ on } \partial D_b. \end{cases}$$

106 It is then easily verified that these functions are eigenvectors of \mathcal{B} -eigenvalues μ_i given by:

$$107 \quad (2.8) \quad \mu_i := -\kappa \langle \partial_\nu w_i, e_i \rangle = \kappa (k^2 \int_{D_b} n |w_i|^2 dx - \int_{D_b} |\nabla w_i|^2 dx).$$

108 In fact, we prove that these are the only possible eigenvalues if k^2 is not a Dirichlet eigenvalue
109 as stated in the following theorem.

110 **Theorem 2.3.** *Assume that k^2 is not an eigenvalue of (2.6), then there are only M non*
111 *zeros real \mathcal{B} -eigenvalues (including multiplicity). These eigenvalues are given by (2.8) (and*
112 *the eigenvectors by (2.7)).*

113 *Proof.* Let μ be an eigenvalue of (2.5) and denote by u its associated eigenvector. From the
114 boundary condition, we deduce that $u|_{\partial D_b} \in \text{span}(e_1, \dots, e_M)$. Since k^2 is not a Dirichlet eigen-
115 value, we deduce that there exists M complex numbers $\alpha_1, \dots, \alpha_M$ such that $u = \sum_{i=1}^M \alpha_i w_i$
116 where the w_i are defined in (2.7). Inserting this expression in the boundary condition, one
117 obtains

$$118 \quad (2.9) \quad \alpha_i (\mu - \mu_i) = 0, \quad i = 1, \dots, M.$$

119 This shows that there exists $i \leq M$ such that $\mu = \mu_i$ (otherwise u would be trivial). ■

120 These \mathcal{B} -eigenvalues corresponds to the values of μ for which one can construct an incident
121 field $u^i \in H^1(D_b)$ solution of $\Delta u^i + k^2 u^i = 0$ in D_b for which $u_b^s = u^s$ in $\mathbb{R}^m \setminus D_b$ where u^s, u_b^s
122 are respectively solutions of (2.1), (2.2). More explicitly, for $\mu = \mu_j$, this incident field is given
123 by $u^i = w_j - u_j^s$ where $u_j^s \in H_{loc}^1(\mathbb{R}^m)$ is the solution of:

$$124 \quad (2.10) \quad \begin{cases} \Delta u_j^s + k^2 u_j^s = k^2 (1 - n) w_j \text{ in } \mathbb{R}^m, \\ \lim_{r \rightarrow +\infty} \int_{|x|=r} \left| \frac{\partial u_j^s}{\partial r} - i k u_j^s \right|^2 = 0. \end{cases}$$

125 **3. The far field operators and statement of the inverse problem.** As indicated above,
126 our goal is to recover some macroscopic properties of the refractive index n from measurements
127 of the scattered field using \mathcal{B} -eigenvalues. The data for this inverse problem is formed by the
128 far fields associated with incident planes waves of the form $u^i(x) = e^{ikx \cdot d}$, denoted $u^i(\cdot, d)$ for
129 $d \in \mathbb{S} := \{x \in \mathbb{R}^m, |x| = 1\}$. Let us denote by $u^s(\cdot, d)$ and $u(\cdot, d)$ the scattered and total field
130 of (2.1) with $u^i = u^i(\cdot, d)$. The scattered field has the following expansion for all $\hat{x} \in \mathbb{S}$,

$$131 \quad u^s(r\hat{x}, d) = \frac{e^{ikr}}{r^{\frac{m-1}{2}}} u^\infty(\hat{x}, d) + O\left(\frac{1}{r^{\frac{m+1}{2}}}\right)$$

132 with $u^\infty(\cdot, d)$ being the so called far field pattern of the scattered field. The data for the
133 inverse problem is constituted by $u^\infty(\hat{x}, d)$ for all $\hat{x}, d \in \mathbb{S}$. Using this data, we define the far
134 field operator $F : L^2(\mathbb{S}) \rightarrow L^2(\mathbb{S})$ by

$$135 \quad (3.1) \quad (Fg)(\hat{x}) := \int_{\mathbb{S}} g(d) u^\infty(\hat{x}, d) ds(d), \quad \hat{x} \in \mathbb{S}.$$

136 We remark that $u_g^\infty := Fg$ is the far field pattern of the scattered field u_g^s , solution of (2.1)
 137 with $u^i = v_g$ the Herglotz wave function defined for $g \in L^2(\mathbb{S})$ by

$$138 \quad (3.2) \quad v_g(x) := \int_{\mathbb{S}} e^{ikxd} g(d) ds(d).$$

139 Introduce the far field constant γ such that

$$140 \quad \gamma := \begin{cases} 4\pi & \text{if } m = 3, \\ e^{-i\frac{\pi}{4}} \sqrt{8\pi k} & \text{if } m = 2. \end{cases}$$

141 We recall that the far field operator F is normal and the scattering operator $S := I + \frac{2ik}{\gamma} F$ is
 142 unitary [16, 21].

143 The algorithm we propose is based on retrieving the \mathcal{B} -eigenvalues from the operator F . This
 144 will be done by incorporating the far field operator associated with the artificial background
 145 defined by (2.2). We therefore similarly introduce the operator $F_b^\mu : L^2(\mathbb{S}) \rightarrow L^2(\mathbb{S})$ defined
 146 by

$$147 \quad (3.3) \quad (F_b^\mu g)(\hat{x}) := \int_{\mathbb{S}} g(d) u_b^\infty(\hat{x}, d) ds(d), \quad \hat{x} \in \mathbb{S},$$

148 where $u_b^\infty(\cdot, d)$ is the far field associated with $u_b^s(\cdot, d)$ the scattered field in (2.2) with $u^i =$
 149 $u^i(\cdot, d)$. This operator is computed numerically or analytically if D_b is a sphere. Then we
 150 define the modified far field operator

$$151 \quad (3.4) \quad \mathcal{F}^\mu := F - F_b^\mu.$$

152 One of the main results of this paper is to show that \mathcal{B} -eigenvalues can be determined by
 153 applying the inside-outside algorithm to the operator

$$154 \quad (3.5) \quad \mathbf{F}^\mu := \gamma S_b^* \mathcal{F}^\mu,$$

155 where $S_b := I + \frac{2ik}{\gamma} F_b^\mu$ is the scattering operator associated with the background. This is done
 156 in the next section. As a preparatory material, we establish first some needed properties of
 157 these far field operators.

158 **3.1. Properties of the far field operators.** We introduce the operator $\mathcal{H}_{\mathcal{B}} : L^2(\mathbb{S}) \rightarrow$
 159 $H^{-\frac{1}{2}}(\partial D_b)$ defined as:

$$160 \quad (3.6) \quad \mathcal{H}_{\mathcal{B}} g := \partial_\nu u_{b,g}|_{\partial D_b},$$

161 where $u_{b,g}$ is solution of (2.2) with $u^i = v_g$, the Herglotz wave function defined in (3.2).

162 For u_g solution of (2.1) with $u^i = v_g$, set

$$163 \quad \begin{cases} w^s := u_g - u_{b,g} & \text{in } \mathbb{R}^m \setminus D_b, \\ w := u_g & \text{in } D_b, \end{cases}$$

164 so that $\mathcal{F}^\mu g = w^\infty$ the far field associated with w^s . By linearity, we obtain that the pair
 165 $(w, w^s) \in H^1(D_b) \times H_{loc}^1(\mathbb{R}^m \setminus D_b)$ is solution of:

$$166 \quad (3.7) \quad \begin{cases} \Delta w + k^2 n w = 0 \text{ in } D_b, \\ \Delta w^s + k^2 w^s = 0 \text{ in } \mathbb{R}^m \setminus D_b, \\ w^s + \frac{1}{\mu} \mathcal{B}(\partial_\nu w^s) = w + \frac{1}{\mu} \mathcal{B}(\partial_\nu w) \text{ on } \partial D_b, \\ \partial_\nu w - \partial_\nu w^s = \psi \text{ on } \partial D_b, \\ \lim_{r \rightarrow +\infty} \int_{|x|=r} \left| \frac{\partial w^s}{\partial r} - i k w^s \right|^2 = 0, \end{cases}$$

167 where $\psi = \partial_\nu u_{b,g}$.

168 The solution of this problem is linear with respect to $\frac{1}{\mu}$. In fact, one can write $w = w_D + \frac{1}{\mu} w_N$
 169 (respectively $w^s = w_D^s + \frac{1}{\mu} w_N^s$) where (w_D, w_D^s) and (w_N, w_N^s) do not depend on μ and are
 170 solution of

$$171 \quad (3.8) \quad \begin{cases} \Delta w_N + k^2 n w_N = 0 \text{ in } D_b, \\ \Delta w_N^s + k^2 w_N^s = 0 \text{ in } \mathbb{R}^m \setminus D_b, \\ w_N - w_N^s = -\mathcal{B}(\psi) \text{ on } \partial D_b, \\ \partial_\nu w_N - \partial_\nu w_N^s = 0 \text{ on } \partial D_b, \\ \lim_{r \rightarrow +\infty} \int_{|x|=r} \left| \frac{\partial w_N^s}{\partial r} - i k w_N^s \right|^2 = 0, \end{cases} \quad \begin{cases} \Delta w_D + k^2 n w_D = 0 \text{ in } D_b, \\ \Delta w_D^s + k^2 w_D^s = 0 \text{ in } \mathbb{R}^m \setminus D_b, \\ w_D - w_D^s = 0 \text{ on } \partial D_b, \\ \partial_\nu w_D - \partial_\nu w_D^s = \psi \text{ on } \partial D_b, \\ \lim_{r \rightarrow +\infty} \int_{|x|=r} \left| \frac{\partial w_D^s}{\partial r} - i k w_D^s \right|^2 = 0. \end{cases}$$

172 **Lemma 3.1.** *Problem (3.7) is well posed for all ψ in $H^{-\frac{1}{2}}(\partial D_b)$. Furthermore, the solution*
 173 *(w, w^s) of (3.7) with source term ψ satisfies the estimate for any compact set Ω that contains*
 174 *D_b :*

$$175 \quad (3.9) \quad \|\Delta w\|_{L^2(D_b)}^2 + \|\Delta w^s\|_{L^2(\Omega \setminus D_b)}^2 + \|w^s\|_{H^1(\Omega \setminus D_b)}^2 + \|w\|_{H^1(D_b)}^2 \leq (C_1 + \frac{1}{\mu} C_2) \|\psi\|_{H^{-\frac{1}{2}}(\partial D_b)}^2,$$

176 where $C_1, C_2 > 0$ do not depend on ψ and μ . In addition, by elliptic regularity, for any
 177 compact set $\Omega \subset \mathbb{R}^m \setminus \overline{D_b}$, there exists a constant $C_b > 0$ independant from ψ such that

$$178 \quad (3.10) \quad \|w^s\|_{H^2(\Omega)}^2 \leq C_b \|\psi\|_{H^{-\frac{1}{2}}(\partial D_b)}^2.$$

179

180 *Proof.* This result is a direct consequence on the well posedness of the problems (3.8) and
 181 the linearity of the solution of (3.7) with respect to $\frac{1}{\mu}$. ■

182 Define the operator $\mathcal{G}_\mathcal{B} : H^{-\frac{1}{2}}(\partial D_b) \rightarrow L^2(\mathbb{S})$ such that: $\mathcal{G}_\mathcal{B}(\psi) := w^\infty$, with w^∞ being
 183 the far field of w^s the solution of (3.7). We then deduce the following factorization:

$$184 \quad (3.11) \quad \mathcal{F}^\mu = \mathcal{G}_\mathcal{B} \mathcal{H}_\mathcal{B}.$$

185 In the following, we shall further expand the factorization of the operator \mathcal{F}^μ and write
 186 it in the form $S_b \mathcal{H}_\mathcal{B}^* T_\mathcal{B} \mathcal{H}_\mathcal{B}$, with a particular operator $T_\mathcal{B}$ whose injectivity is related to the
 187 \mathcal{B} -eigenvalues. We first state a lemma that characterizes the adjoint of $\mathcal{H}_\mathcal{B}$ denoted by
 188 $\mathcal{H}_\mathcal{B}^* : H^{\frac{1}{2}}(\partial D_b) \rightarrow L^2(\mathbb{S})$.

189 **Lemma 3.2.** *The operator $\mathcal{H}_{\mathcal{B}}$ is injective and its range is dense in $H^{-\frac{1}{2}}(\partial D_b)$. Moreover,*
 190 *the adjoint operator $\mathcal{H}_{\mathcal{B}}^*$ is defined by: $\mathcal{H}_{\mathcal{B}}^*\phi = \gamma S_b^* \tilde{w}^\infty$ for all $\phi \in H^{\frac{1}{2}}(\partial D_b)$, where \tilde{w}^∞ is the*
 191 *far field pattern of $\tilde{w} \in H_{loc}^1(\mathbb{R}^m \setminus D_b)$ solution of:*

$$192 \quad (3.12) \quad \begin{cases} \Delta \tilde{w} + k^2 \tilde{w} = 0 \text{ in } \mathbb{R}^m \setminus D_b, \\ \tilde{w} + \frac{1}{\mu} \mathcal{B}(\partial_\nu \tilde{w}) = \phi \text{ on } \partial D_b, \\ \lim_{r \rightarrow +\infty} \int_{|x|=r} \left| \frac{\partial \tilde{w}}{\partial r} - ik\tilde{w} \right|^2 = 0. \end{cases}$$

193 *Proof.* We first prove the last part of the lemma. Let $g \in L^2(\mathbb{S})$. Applying Green's formula
 194 twice, one obtains

$$195 \quad (3.13) \quad \begin{aligned} 0 &= \int_{B_R \setminus D_b} (\Delta \tilde{w} + k^2 \tilde{w}) u_{b,g}^s dx \\ &= \int_{\partial B_R} (\partial_\nu \tilde{w} u_{b,g}^s - \tilde{w} \partial_\nu u_{b,g}^s) ds - \int_{\partial D_b} (\partial_\nu \tilde{w} u_{b,g} - \tilde{w} \partial_\nu u_{b,g}) ds \\ &\quad + \int_{\partial D_b} (\partial_\nu \tilde{w} v_g - \tilde{w} \partial_\nu v_g) ds. \end{aligned}$$

196 Using the Sommerfeld radiation condition, one gets

$$197 \quad (3.14) \quad \lim_{R \rightarrow +\infty} \int_{\partial B_R} (\partial_\nu \tilde{w} u_{b,g}^s - \tilde{w} \partial_\nu u_{b,g}^s) ds = -2ik \int_{\mathbb{S}} \overline{\tilde{w}^\infty}(d) u_{b,g}^\infty(d) ds(d).$$

198 We recall that the far field \tilde{w}^∞ admits the following expression:

$$199 \quad (3.15) \quad \gamma \tilde{w}^\infty(d) = - \int_{\partial D_b} (\partial_{\nu(x)} \tilde{w}(x) e^{-ikx \cdot d} - \partial_{\nu(x)} e^{-ikx \cdot d} \tilde{w}) ds(x).$$

200 Thus, replacing v_g by its expression, one obtains:

$$201 \quad (3.16) \quad -\bar{\gamma} \int_{\mathbb{S}} g(d) \overline{\tilde{w}^\infty(d)} ds = \int_{\partial D_b} (\partial_\nu \tilde{w} v_g - \tilde{w} \partial_\nu v_g) ds.$$

202 Using the boundary condition of \tilde{w} and $u_{b,g}$, we deduce that

$$203 \quad (3.17) \quad \begin{aligned} \int_{\partial D_b} (\partial_\nu \tilde{w} u_{b,g} - \tilde{w} \partial_\nu u_{b,g}) ds &= \int_{\partial D_b} (\partial_\nu \tilde{w} (-\frac{1}{\mu} \mathcal{B}(\partial_\nu u_{b,g})) - \tilde{w} \partial_\nu u_{b,g}) ds \\ &= - \int_{\partial D_b} \partial_\nu u_{b,g} \bar{\phi} ds, \end{aligned}$$

204 where, for the last equality we used the fact that \mathcal{B} is self-adjoint. Equations (3.13), (3.14),
 205 (3.16) and (3.17) give

$$206 \quad (3.18) \quad \int_{\partial D_b} \partial_\nu u_{b,g} \bar{\phi} ds = 2ik \int_{\mathbb{S}} \overline{\tilde{w}^\infty}(d) u_{b,g}^\infty(d) ds(d) + \bar{\gamma} \int_{\mathbb{S}} g(d) \overline{\tilde{w}^\infty(d)} ds.$$

207 Hence, using the definition of $\mathcal{H}_{\mathcal{B}}$, we get:

$$208 \quad (3.19) \quad \begin{aligned} \langle \mathcal{H}_{\mathcal{B}} g, \phi \rangle_{H^{-\frac{1}{2}}(\partial D_b), H^{\frac{1}{2}}(\partial D_b)} &= \bar{\gamma} (g, \tilde{w}^\infty)_{L^2(\mathbb{S})} + 2ik (F^b g, \tilde{w}^\infty) \\ &= \bar{\gamma} (S_b g, \tilde{w}^\infty)_{L^2(\mathbb{S})}. \end{aligned}$$

209 We then conclude that $\mathcal{H}_{\mathcal{B}}^* \phi = \gamma S_b^* \tilde{w}^\infty$.

210 We now prove the injectivity of $\mathcal{H}_{\mathcal{B}}$. Assume that $\mathcal{H}_{\mathcal{B}} g = 0$ for some $g \in L^2(\mathbb{S})$. This implies
 211 in particular that $\partial_\nu u_{b,g}|_{\partial D_b} = 0$ and $u_{b,g}$ vanishes on ∂D_b by the boundary condition, which
 212 gives $u_{b,g}^s = -v_g$ in $\mathbb{R}^m \setminus D_b$. Therefore the Herglotz wave function v_g which satisfies the
 213 Helmholtz equation in \mathbb{R}^m also satisfies the radiation condition. This proves that $v_g = 0$ and
 214 then $g = 0$ ([16]).

215 We know prove that $\mathcal{H}_{\mathcal{B}}$ has dense range by showing that $\mathcal{H}_{\mathcal{B}}^*$ is injective. If $\mathcal{H}_{\mathcal{B}}^* \phi = 0$ then
 216 $\gamma S_b^* \tilde{w}^\infty = 0$ for some $\phi \in H^{\frac{1}{2}}(\partial D_b)$. Using Rellich's lemma and the fact that S_b^* is unitary
 217 (see Proposition B.2) and therefore injective, we infer that only $\phi = 0$ satisfies the equality. ■

218 The previous lemma implies in particular that $S_b \mathcal{H}_{\mathcal{B}}^* \phi = \gamma \tilde{w}^\infty$. Let us introduce the operator
 219 $T_{\mathcal{B}} : H^{-\frac{1}{2}}(\partial D_b) \rightarrow H^{\frac{1}{2}}(\partial D_b)$ defined by

$$220 \quad (3.20) \quad T_{\mathcal{B}}(\psi) = w + \frac{1}{\mu} \mathcal{B}(\partial_\nu w) = w^s + \frac{1}{\mu} \mathcal{B}(\partial_\nu w^s)$$

221 where (w, w^s) is the unique solution of (3.7). We then have $\mathcal{G}_{\mathcal{B}} \psi = S_b \mathcal{H}_{\mathcal{B}}^* T_{\mathcal{B}} \psi$. We deduce
 222 from (3.11) that \mathcal{F}^μ assumes the following factorization:

$$223 \quad (3.21) \quad \gamma \mathcal{F}^\mu = S_b \mathcal{H}_{\mathcal{B}}^* T_{\mathcal{B}} \mathcal{H}_{\mathcal{B}}.$$

224 Using the fact that S_b is unitary (see Proposition B.2 in B), we infer that

$$225 \quad (3.22) \quad \mathbf{F} = \mathcal{H}_{\mathcal{B}}^* T_{\mathcal{B}} \mathcal{H}_{\mathcal{B}}.$$

226 In addition, let us also observe that the operator $\mathbf{S} := I + \frac{2ik}{|\gamma|^2} \mathbf{F}$ is unitary due to the fact
 227 that S and S_b are unitary. This also implies in particular that \mathbf{F} is a normal operator.

228 **4. The inside-outside duality applied to \mathbf{F} .** Consider the case where $\mu \neq 0$ is not a
 229 \mathcal{B} -eigenvalue. Since \mathbf{F} is a compact and normal operator, there exists an orthonormal com-
 230 plete basis $(g_j)_{j \in \mathbb{N}}$ of $L^2(\mathbb{S})$ such that $\mathbf{F} g_j = \lambda_j g_j$ where $(\lambda_j)_{j \in \mathbb{N}}$ are the eigenvalues of \mathbf{F} that
 231 accumulate at 0.

232 Exploiting the fact that \mathbf{S} is unitary, we deduce that the eigenvalues of \mathbf{F} lie on the circle
 233 of radius $\frac{|\gamma|^2}{2k}$ and center $\frac{|\gamma|^2}{2ik}$. We set $\lambda_j := \frac{|\gamma|^2}{2ik} (e^{i\delta_j} - 1)$ with $e^{i\delta_j}$ being an eigenvalue of \mathbf{S} ,
 234 $\delta_j \in [0, 2\pi)$ and define

$$235 \quad (4.1) \quad \begin{cases} \delta_*(\mu) & := \max_{j \geq 1} \delta_j, \\ \lambda_* & := \frac{|\gamma|^2}{2ik} (e^{i\delta_*} - 1). \end{cases}$$

236 We then can state the main theorem of this section:

237 **Theorem 4.1.** *Assume that k^2 is not an eigenvalue of (2.6). μ_0 is a \mathcal{B} -eigenvalue if and*
 238 *only if $\delta_*(\mu) \rightarrow 2\pi$ as $\mu \rightarrow \mu_0$ with $\mu > \mu_0$.*

239 This theorem is a straightforward corollary of Proposition 4.6 (sufficient condition) and Propo-
 240 sition 4.8 (necessary condition). In order to prove these propositions, we first establish some
 241 properties of the operator $T_{\mathcal{B}}$ in the factorization (3.22).

242 **4.1. Some key properties of the operator $T_{\mathcal{B}}$.** One of the important ingredients of the
 243 inside-outside duality is the link between the kernel of the operator $T_{\mathcal{B}}$ and the \mathcal{B} -eigenvalues.
 244 The latter is proved in the following lemmas.

245
 246 To shorten the notations, the duality product $\langle \cdot, \cdot \rangle_{H^{\frac{1}{2}}(\partial D_b), H^{-\frac{1}{2}}(\partial D_b)}$ will be denoted $\langle \cdot, \cdot \rangle$
 247 or in an abuse of notation as an integral over ∂D_b .

248 **Lemma 4.2.** *The operator $T_{\mathcal{B}}$ satisfies the energy identity:*

$$249 \quad (4.2) \quad \Im \langle T_{\mathcal{B}}\psi, \psi \rangle = k \int_{\mathbb{S}} |w^\infty|^2 ds, \quad \forall \psi \in H^{-\frac{1}{2}}(\partial D_b),$$

250 where w^∞ is the far field pattern of w^s , with (w, w^s) being the solution of (3.7) with source
 251 term ψ .

252 *Proof.* Let $\psi \in H^{-\frac{1}{2}}(\partial D_b)$, using that $\psi = \partial_\nu w - \partial_\nu w^s$, we get

$$253 \quad (4.3) \quad \langle T_{\mathcal{B}}\psi, \psi \rangle = \int_{\partial D_b} \partial_\nu \bar{w} (w + \frac{1}{\mu} \mathcal{B}(\partial_\nu w)) ds - \int_{\partial D_b} \partial_\nu \bar{w}^s (w^s + \frac{1}{\mu} \mathcal{B}(\partial_\nu w^s)) ds.$$

254 Let us focus on the last term of the previous equality. Using Green's formula on a ball B_R of
 255 radius $R > 0$ large enough, one obtains:

$$\begin{aligned} 256 \quad (4.4) \quad 0 &= - \int_{B_R \setminus D_b} w^s (\Delta \bar{w}^s + k^2 n \bar{w}^s) dx \\ &= \int_{B_R \setminus D_b} |\nabla w^s|^2 dx - k^2 \int_{B_R \setminus D_b} n |w^s|^2 dx \\ &\quad + ik \int_{\partial B_R} |w^s|^2 ds - \int_{\partial B_R} (\partial_\nu \bar{w}^s + ik \bar{w}^s) w^s ds \\ &\quad + \int_{\partial D_b} \partial_\nu \bar{w}^s w^s ds. \end{aligned}$$

257 Substituting the expression of $\int_{\partial D_b} \partial_\nu \bar{w}^s w^s ds$ in (4.3) gives

$$\begin{aligned} 258 \quad (4.5) \quad \langle T_{\mathcal{B}}\psi, \psi \rangle &= \int_{\partial D_b} \partial_\nu \bar{w} w ds \\ &\quad + \int_{B_R \setminus D_b} |\nabla w^s|^2 dx - k^2 \int_{B_R \setminus D_b} n |w^s|^2 dx \\ &\quad + ik \int_{\partial B_R} |w^s|^2 ds - \int_{\partial B_R} (\partial_\nu \bar{w}^s + ik \bar{w}^s) w^s ds \\ &\quad + \frac{1}{\mu} \int_{\partial D_b} \mathcal{B}(\partial_\nu w) \partial_\nu \bar{w} - \frac{1}{\mu} \int_{\partial D_b} \mathcal{B}(\partial_\nu w^s) \partial_\nu \bar{w}^s. \end{aligned}$$

259 Taking the imaginary part of this equality while letting $R \rightarrow +\infty$, we obtain

$$\begin{aligned} 260 \quad (4.6) \quad \Im \langle T_{\mathcal{B}}\psi, \psi \rangle &= k \int_{\mathbb{S}} |w^\infty|^2 ds + \Im \int_{\partial D_b} \partial_\nu \bar{w} w ds, \\ &= k \int_{\mathbb{S}} |w^\infty|^2 ds - k^2 \int_{D_b} \Im(n) |w|^2 dx, \end{aligned}$$

261 where for the last equality, we used that $\Delta w + k^2 n w = 0$ in D_b . ■

262 **Proposition 4.3.** *Let $\mu \in \mathbb{R}^*$. μ is a \mathcal{B} -eigenvalue if and only if there exists a non trivial
 263 $\psi \in H^{-\frac{1}{2}}(\partial D_b)$ such that $\Im \langle T_{\mathcal{B}}\psi, \psi \rangle = 0$.*

264 *Proof.* Assume that μ is a \mathcal{B} -eigenvalue. We denote by $w_0 \in H^1(D_b)$ its associated
 265 eigenvector. Set $\psi = \partial_\nu w_0|_{\partial D_b}$ which is necessarily non trivial. Consider (w, w^s) the associated
 266 solution of (3.7). We then get thanks to Green's theorem:

$$\begin{aligned} \langle T_{\mathcal{B}}\psi, \psi \rangle &= \int_{\partial D_b} w \partial_\nu \overline{w_0} ds + \frac{1}{\mu} \int_{\partial D_b} \partial_\nu \overline{w_0} \mathcal{B}(\partial_\nu w) ds \\ (4.7) \quad &= \int_{\partial D_b} \overline{w_0} \partial_\nu w ds + \frac{1}{\mu} \int_{\partial D_b} \partial_\nu w \mathcal{B}(\partial_\nu \overline{w_0}) ds = 0, \end{aligned}$$

268 where we used the fact that \mathcal{B} is self-adjoint and the fact w, w_0 verify the same inhomogeneous
 269 Helmholtz equation in D_b . Conversely, assume there exists $\psi \in H^{-\frac{1}{2}}(\partial D_b)$ non trivial such
 270 that $\Im m \langle T_{\mathcal{B}}\psi, \psi \rangle = 0$. By Rellich lemma, this implies $w^s = 0$ in $\mathbb{R}^m \setminus D_b$ where (w, w^s) is
 271 the solution of (3.7) with source term ψ . In particular, we get $w^s|_{\partial D_b} = 0$ and $\partial_\nu w^s|_{\partial D_b} = 0$.
 272 Thus, μ is a \mathcal{B} -eigenvalue associated with the non trivial eigenvector w . \blacksquare

273 We conclude this section by showing that $T_{\mathcal{B}}$ is a Fredholm operator of index 0.

274 **Lemma 4.4.** *$T_{\mathcal{B}}$ admits the following decomposition*

$$275 \quad T_{\mathcal{B}} = T_0 + K,$$

276 where K is compact and T_0 is coercive. More precisely, there exists $\alpha > 0$ such that

$$277 \quad (4.8) \quad \langle T_0\psi, \psi \rangle \geq \alpha \|\psi\|_{H^{-\frac{1}{2}}(\partial D_b)}^2.$$

278

279 *Proof.* Let $\psi, \psi' \in H^{-\frac{1}{2}}(\partial D_b)$ and (w, w^s) (respectively (w', w'^s)) the solution of (3.7)
 280 with source term ψ (respectively ψ'). Exploiting the definition of $T_{\mathcal{B}}$, one can deduce:

$$\begin{aligned} \langle T_{\mathcal{B}}\psi, \psi' \rangle &= \int_{\partial D_b} \overline{\psi'} (w + \frac{1}{\mu} \mathcal{B}(\partial_\nu w)) ds = \int_{\partial D_b} \overline{\psi'} (w^s + \frac{1}{\mu} \mathcal{B}(\partial_\nu w^s)) ds, \\ (4.9) \quad &= \int_{\partial D_b} \partial_\nu \overline{w'} w ds - \int_{\partial D_b} \partial_\nu \overline{w'^s} w^s ds \\ &+ \frac{1}{\mu} \int_{\partial D_b} \partial_\nu \overline{w'} \mathcal{B}(\partial_\nu w) ds - \frac{1}{\mu} \int_{\partial D_b} \partial_\nu \overline{w'^s} \mathcal{B}(\partial_\nu w^s) ds. \end{aligned}$$

282 Let B_R be a ball containing D_b for R large enough. We define the operator $T_0 : H^{-\frac{1}{2}}(\partial D_b) \rightarrow$
 283 $H^{\frac{1}{2}}(\partial D_b)$ as:

$$\begin{aligned} \langle T_0\psi, \psi' \rangle &= \int_{B_R \setminus D_b} \nabla w^s \nabla \overline{w'^s} dx + \int_{B_R \setminus D_b} w^s \overline{w'^s} dx \\ (4.10) \quad &+ \int_{D_b} \nabla w \nabla \overline{w'} dx + \int_{D_b} w \overline{w'} dx, \end{aligned}$$

285 and $K : H^{-\frac{1}{2}}(\partial D_b) \rightarrow H^{\frac{1}{2}}(\partial D_b)$ as:

$$\begin{aligned} \langle K\psi, \psi' \rangle &= -(1 + k^2) \int_{B_R \setminus D_b} w^s \overline{w'^s} dx \\ &- (1 + k^2) \int_{D_b} n w \overline{w'} dx \\ (4.11) \quad &- \int_{\partial B_R} \partial_\nu \overline{w'^s} w^s ds \\ &+ \frac{1}{\mu} \int_{\partial D_b} \partial_\nu \overline{w'} \mathcal{B}(\partial_\nu w) ds - \frac{1}{\mu} \int_{\partial D_b} \partial_\nu \overline{w'^s} \mathcal{B}(\partial_\nu w^s) ds. \end{aligned}$$

287 Thus, one can write $T_{\mathcal{B}} = T_0 + K$.

288 Since $\psi = \partial_\nu w - \partial_\nu w^s$, we deduce that

$$\begin{aligned}
 \|\psi\|_{H^{-\frac{1}{2}}(\partial D_b)}^2 &\leq 2(\|\partial_\nu w\|_{H^{-\frac{1}{2}}(\partial D_b)}^2 + \|\partial_\nu w^s\|_{H^{-\frac{1}{2}}(\partial D_b)}^2), \\
 (4.12) \quad &\leq 2(\|\nabla w\|_{L^2(D_b)}^2 + \|\Delta w\|_{L^2(D_b)}^2 \\
 &\quad + \|\nabla w^s\|_{L^2(B_R \setminus D_b)}^2 + \|\Delta w^s\|_{L^2(B_R \setminus D_b)}^2).
 \end{aligned}$$

290 Using the fact that w and w^s satisfy the Helmholtz equation, one can therefore deduce the
 291 existence of some $\alpha > 0$ such that

$$\begin{aligned}
 \alpha \|\psi\|_{H^{-\frac{1}{2}}(\partial D_b)}^2 &\leq (\|w\|_{H^1(D_b)}^2 + \|w^s\|_{H^1(B_R \setminus D_b)}^2), \\
 (4.13) \quad &= \langle T_0 \psi, \psi \rangle.
 \end{aligned}$$

293 The compactness of the operator K is a direct consequence of a priori estimates in Lemma 3.1,
 294 trace theorems, Rellich's compact embedding theorems and the compactness of the operator
 295 \mathcal{B} . ■

296 One of the consequences of the previous decomposition of $T_{\mathcal{B}}$ in Lemma 4.4 is that if μ is
 297 not a \mathcal{B} -eigenvalue, the eigenvalues λ_j of the operator \mathbf{F} accumulate at 0 from the right, that
 298 is $\Re(\lambda_j) > 0$ for j large enough ([21, 22]). This is equivalent to say that δ_j (the argument of
 299 λ_j) converges to 0 as j goes to $+\infty$. In contrast, Theorem 4.1 states that when μ approaches
 300 a \mathcal{B} -eigenvalue, the eigenvalue $\lambda_*(\mu)$ approaches 0 from the left as illustrated in Figure 1. In
 301 addition, if μ is not a \mathcal{B} -eigenvalue, Lemma 6 and 8 imply $T_{\mathcal{B}}$ is coercive [21], that is there
 302 exists a constant $\alpha > 0$ such that for all $\psi \in H^{-\frac{1}{2}}(\partial D_b)$

$$(4.14) \quad |\langle T_{\mathcal{B}} \psi, \psi \rangle| \geq \alpha \|\psi\|_{H^{-\frac{1}{2}}(\partial D_b)}^2.$$

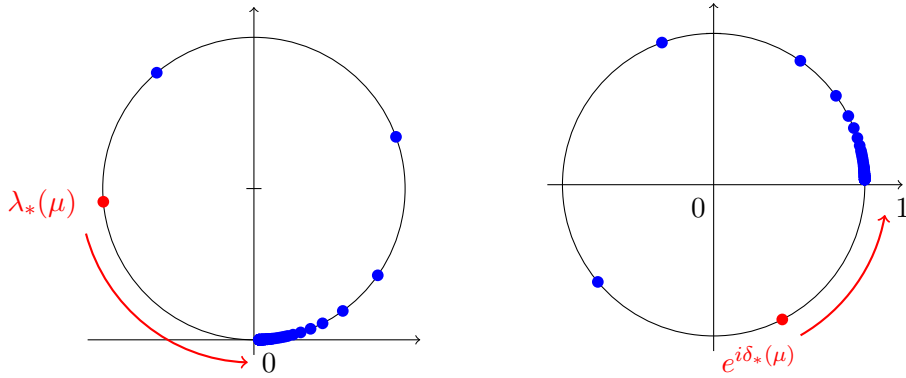


Figure 1. Illustration of Theorem 4.1. Left: The eigenvalues of \mathbf{F} accumulates at 0 from the right (in blue) while $\lambda_*(\mu)$ (in red) approaches 0 from the left as μ approaches the \mathcal{B} -eigenvalue. Right: The argument of the eigenvalues of \mathbf{S} accumulates at 0 (in blue) while $\delta_*(\mu)$ (in red) approaches 2π as μ approaches the \mathcal{B} -eigenvalue.

304 We dedicate the two next subsections to the proof of Theorem 4.1.

305 **4.2. Proof of the sufficient condition in Theorem 4.1.** Since we will be dealing with
 306 convergence of sequences that depend on μ , we shall explicitly indicate the dependence
 307 on μ in the notation for the operators (in particular, the operator $\mathbf{F}(\mu)$ is factorized as
 308 $\mathcal{H}_{\mathcal{B}}^*(\mu)T_{\mathcal{B}}(\mu)\mathcal{H}_{\mathcal{B}}(\mu)$).
 309

310 **Proposition 4.5.** *The mapping $\mu \rightarrow T_{\mathcal{B}}(\mu)$ is continuous from \mathbb{R}^* to the space of linear
 311 bounded operators from $H^{-\frac{1}{2}}(\partial D_b)$ to $H^{\frac{1}{2}}(\partial D_b)$ endowed with the usual operator norm.*

312 *Proof.* The proof is a direct consequence of the linear dependence with respect to $\frac{1}{\mu}$ of the
 313 solution (w, w^s) of problem (3.7) (see 18) and the expression of $T_{\mathcal{B}}(\mu)$. \blacksquare

314 **Proposition 4.6.** *Let $\mu_0 \in \mathbb{R}^*$ and $I = (\mu_0 - \varepsilon, \mu_0 + \varepsilon) \setminus \{\mu_0\}$ for some $\varepsilon > 0$ sufficiently
 315 small such that no $\mu \in I$ is a \mathcal{B} -eigenvalue and such that $0 \notin I$. Assume there is a sequence
 316 $(\mu_j)_j$ of elements of I such that*

$$317 \quad \mu_j \longrightarrow \mu_0 \quad \text{and} \quad \delta_*(\mu_j) \longrightarrow 2\pi.$$

318 *Then μ_0 is a \mathcal{B} -eigenvalue.*

319 *Proof.* Consider the sequence $\varphi_j = \frac{1}{\sqrt{|\lambda_*|}} \mathcal{H}_{\mathcal{B}}(\mu_j)g_j$, where g_j is the normalized eigenvector
 320 of $\mathbf{F}(\mu_j)$ associated with $\lambda_*(\mu_j)$. We then have by assumptions

$$321 \quad (4.15) \quad \langle T_{\mathcal{B}}(\mu_j)\varphi_i, \varphi_i \rangle = \frac{\lambda_*(\mu_j)}{|\lambda_*(\mu_j)|} \longrightarrow_{j \rightarrow +\infty} -1.$$

322 Assume by contradiction that μ_0 is not a \mathcal{B} -eigenvalue.

323 In that case, the operator $T_{\mathcal{B}}(\mu_j)$ is coercive for every $\mu_j \in I$. Using that $\mu \rightarrow T_{\mathcal{B}}(\mu)$ is
 324 continuous in the operator norm, we infer that the coercivity constant can be chosen inde-
 325 pendent from $\mu \in \bar{I}$. The coercivity of $T_{\mathcal{B}}(\mu_j)$ and identity (4.15) show that $(\varphi_j)_j$ is bounded
 326 and therefore weakly converges (up to a subsequence) to some φ_0 in $H^{-\frac{1}{2}}(\partial D_b)$. Denote by
 327 (w_j, w_j^s) (respectively (w_0, w_0^s)) the solution of (3.7) with $\psi = \varphi_j$ (respectively $\psi = \varphi_0$). From
 328 Lemma 4.2, one gets:

$$329 \quad (4.16) \quad \Im m \langle T_{\mathcal{B}}(\mu_j)\varphi_j, \varphi_j \rangle = k \int_{\mathbb{S}} |w_j^\infty|^2 ds.$$

330 Since the application $\psi \in H^{-\frac{1}{2}}(\partial D_b) \rightarrow w^\infty(\psi) \in L^2(\mathbb{S})$ (where $w^\infty(\psi)$ is the far field pattern
 331 of w^s solution of (3.7) with source term ψ) is compact, then $\Im m \langle T_{\mathcal{B}}(\mu_j)\varphi_j, \varphi_j \rangle$ converges to
 332 $\Im m \langle T_{\mathcal{B}}(\mu_0)\varphi_0, \varphi_0 \rangle$. Identity (4.15) implies that $\lim_{j \rightarrow +\infty} \Im m \langle T_{\mathcal{B}}(\mu_j)\varphi_j, \varphi_j \rangle = 0$ and therefore
 333 $\varphi_0 = 0$ by Proposition 4.3.

334 Recall that $T_{\mathcal{B}}(\mu_j)$ assumes the decomposition $T_{\mathcal{B}}(\mu_j) = T_0(\mu_j) + K(\mu_j)$, where $T_0(\mu_j)$ is real
 335 coercive and $K(\mu_j)$ is compact. Let us show that $\lim_{j \rightarrow +\infty} \langle K(\mu_j)\varphi_j, \varphi_j \rangle = 0$. From the

336 decomposition shown in Lemma 4.4, we get that

$$\begin{aligned}
 \langle K(\mu_j)\varphi_j, \varphi_j \rangle &= -(1+k^2)\|w_j^s\|_{H^1(B_R \setminus D_b)}^2 \\
 &\quad -(1+k^2)(nw_j, w_j)_{H^1(D_b)} \\
 337 \quad (4.17) \quad &\quad - \int_{\partial B_R} \partial_\nu \overline{w_j^s} w_j^s ds \\
 &\quad + \frac{1}{\mu_j} \int_{\partial D_b} \partial_\nu \overline{w_j^s} \mathcal{B}(\partial_\nu w_j) ds - \frac{1}{\mu_j} \int_{\partial D_b} \partial_\nu \overline{w_j^s} \mathcal{B}(\partial_\nu w_j^s) ds.
 \end{aligned}$$

338 The first three terms converge to 0 by the same arguments as in the proof of the compactness
 339 of $K(\mu_j)$ for μ_j fixed in Lemma 4.4. We conclude in the same way for the last two terms using
 340 that the sequence $\frac{1}{\mu_j}$ converges to $\frac{1}{\mu_0}$. This shows that $\lim_{j \rightarrow +\infty} \langle K(\mu_j)\varphi_j, \varphi_j \rangle = 0$.

341 We deduce that (up to a subsequence) $\langle T_0(\mu_j)\varphi_j, \varphi_j \rangle$ converges to -1 which is a contradiction
 342 since $\langle T_0(\mu_j)\varphi_j, \varphi_j \rangle \geq 0$ for all $j \in \mathbb{N}$ (Lemma 4.4). ■

343 **4.3. Proof of the necessary condition in Theorem 4.1.** For the proof of the necessary
 344 condition, we use the Cayley transform associated with \mathbf{S} ([22]).

345 Assume that μ is not a \mathcal{B} -eigenvalue. Then 1 is not an eigenvalue of \mathbf{S} because \mathbf{F} is injective
 346 and we can define the Cayley transform:

$$347 \quad \mathcal{T} := i(Id + \mathbf{S})(Id - \mathbf{S})^{-1}.$$

348 \mathcal{T} is self-adjoint and has a discrete spectrum. We have the equivalence $e^{i\delta_*}$ is an eigenvalue
 349 of \mathbf{S} if and only if $\cot(\delta_*/2) \in \mathbb{R}$ is an eigenvalue of \mathcal{T} . Applying Courant Fischer min max
 350 principle to \mathcal{T} , we get:

$$351 \quad (4.18) \quad \cot(\delta_*/2) = \inf_{\psi \in H^{-\frac{1}{2}}(\partial D_b)} \frac{\Re \langle \mathcal{T}\psi, \psi \rangle}{\Im m \langle \mathcal{T}\psi, \psi \rangle}.$$

352 Let μ_0 be a \mathcal{B} -eigenvalue associated with the eigenvector w_0 . For $\mu \in \mathbb{R}^*$, define
 353 $(w(\mu), w^s(\mu))$ the solution of (3.7) with source term $\psi = \partial_\nu w_0$. From the linearity of those
 354 solutions with respect to $\frac{1}{\mu}$ (see decomposition (3.8)), one can obtain the following expansion:
 355

$$356 \quad (4.19) \quad w(\mu) - w_0 = \left(\frac{1}{\mu} - \frac{1}{\mu_0}\right)w_N^0,$$

357 where w_N^0 does not depend on μ and is solution of (3.8) with $\psi = \partial_\nu w_0$.

358 **Proposition 4.7.** Let μ_0 be a \mathcal{B} -eigenvalue associated with w_0 . For $\mu \in \mathbb{R}^*$, define
 359 $(w(\mu), w^s(\mu))$ the solution of (3.7) with source term $\psi = \partial_\nu w_0$ and parameter μ . Then :

$$360 \quad (4.20) \quad \langle T_{\mathcal{B}}(\mu)\partial_\nu w_0, \partial_\nu w_0 \rangle = \left(\frac{1}{\mu} - \frac{1}{\mu_0}\right) \langle \mathcal{B}(\partial_\nu w_0), \partial_\nu w_0 \rangle + \left(\frac{1}{\mu} - \frac{1}{\mu_0}\right)^2 \langle \mathcal{B}(\partial_\nu w_N^0), \partial_\nu w_0 \rangle.$$

361 *Proof.* According to the definition of $T_{\mathcal{B}}(\mu)$, we get:

$$362 \quad (4.21) \quad \langle T_{\mathcal{B}}(\mu)\partial_\nu w_0, \partial_\nu w_0 \rangle = \left\langle w(\mu) + \frac{1}{\mu} \mathcal{B}(\partial_\nu w(\mu)), \partial_\nu w_0 \right\rangle.$$

363 Since $-\langle T_{\mathcal{B}}(\mu_0)\partial_\nu w_0, \partial_\nu w_0 \rangle = 0$, we can add it to the previous equality and by rearranging
 364 the terms, one has

$$365 \quad \langle T_{\mathcal{B}}(\mu)\partial_\nu w_0, \partial_\nu w_0 \rangle = \left\langle w(\mu) - w_0 + \frac{1}{\mu}\mathcal{B}(\partial_\nu w(\mu) - \partial_\nu w_0), \partial_\nu w_0 \right\rangle + \left(\frac{1}{\mu} - \frac{1}{\mu_0}\right) \langle \mathcal{B}(\partial_\nu w_0), \partial_\nu w_0 \rangle.$$

366 The previous equality can be rewritten using (4.19) as:

$$367 \quad (4.22) \quad \langle T_{\mathcal{B}}(\mu)\partial_\nu w_0, \partial_\nu w_0 \rangle = \left(\frac{1}{\mu} - \frac{1}{\mu_0}\right) \left(\left\langle w_N^0 + \frac{1}{\mu}\mathcal{B}(\partial_\nu w_N^0), \partial_\nu w_0 \right\rangle + \langle \mathcal{B}(\partial_\nu w_0), \partial_\nu w_0 \rangle \right).$$

368 Using Green's theorem, we have:

$$369 \quad \begin{aligned} 0 &= -\int_{D_b} (\Delta w_N^0 + k^2 n w_N^0) \overline{w_0} dx = \int_{\partial D_b} (\partial_\nu \overline{w_0} w_N^0 - \partial_\nu w_N^0 \overline{w_0}) ds \\ &= \left\langle w_N^0 + \frac{1}{\mu_0}\mathcal{B}(\partial_\nu w_N^0), \partial_\nu w_0 \right\rangle. \end{aligned}$$

370 Expression (4.20) is obtained by substituting $\langle w_N^0, \partial_\nu w_0 \rangle$ in (4.22). ■

371 We possess all the ingredients to prove the following necessary condition.

372 **Proposition 4.8.** *Assume that μ_0 is a \mathcal{B} -eigenvalue and k^2 is not an eigenvalue of (2.6).
 373 Then $\delta_*(\mu) \rightarrow 2\pi$ as $\mu \rightarrow \mu_0$ with $\mu > \mu_0$.*

374 *Proof.* The proof uses the positiveness of the \mathcal{B} operator. Let us first show that the first
 375 term in the decomposition (4.20) is non zero. Assume by contradiction that $\langle \mathcal{B}(\partial_\nu w_0), \partial_\nu w_0 \rangle =$
 376 0 . Using the form of \mathcal{B} in (2.3), one has that $\langle \partial_\nu w_0, e_i \rangle = 0$ for all $i \leq M$ which implies
 377 $\mathcal{B}(\partial_\nu w_0) = 0$. Using that $\mu_0 \neq 0$, one obtains thanks to the boundary condition that $w_0|_{\partial D_b} =$
 378 0 which contradicts the assumption on k^2 . Hence, we have $\langle \mathcal{B}(\partial_\nu w_0), \partial_\nu w_0 \rangle > 0$.

379 Let μ_0 be a \mathcal{B} -eigenvalue associated with the eigenvector w_0 . Then we have for μ in a
 380 neighborhood of μ_0 :

$$381 \quad (4.23) \quad \cot(\delta_*(\mu)/2) = \inf_{\psi \in H^{-\frac{1}{2}}(\partial D_b)} \frac{\Re \langle T_{\mathcal{B}}(\mu)\psi, \psi \rangle}{\Im m \langle T_{\mathcal{B}}(\mu)\psi, \psi \rangle} \leq \frac{\Re \langle T_{\mathcal{B}}(\mu)\partial_\nu w_0, \partial_\nu w_0 \rangle}{\Im m \langle T_{\mathcal{B}}(\mu)\partial_\nu w_0, \partial_\nu w_0 \rangle}$$

382 with $\Im m \langle T_{\mathcal{B}}(\mu)\partial_\nu w_0, \partial_\nu w_0 \rangle > 0$ thanks to Lemma 4.2. From the previous Lemma, we con-
 383 clude that:

$$384 \quad \frac{\Re \langle T_{\mathcal{B}}(\mu)\partial_\nu w_0, \partial_\nu w_0 \rangle}{\Im m \langle T_{\mathcal{B}}(\mu)\partial_\nu w_0, \partial_\nu w_0 \rangle} = \frac{\langle \mathcal{B}(\partial_\nu w_0), \partial_\nu w_0 \rangle + \left(\frac{1}{\mu} - \frac{1}{\mu_0}\right) \Re e(\langle \mathcal{B}(\partial_\nu w_N^0), \partial_\nu w_0 \rangle)}{\left(\frac{1}{\mu} - \frac{1}{\mu_0}\right) \Im m \langle T_{\mathcal{B}}(\mu)\partial_\nu w_0, \partial_\nu w_0 \rangle} \rightarrow -\infty,$$

385 as $\mu \rightarrow \mu_0$ with $\mu > \mu_0$. Combined with (4.23), this proves the claim of the proposition. ■

386 We end this section by a result that indicates how one can also recover an eigenvector w_0
 387 associated with μ . The proof is similar to the one in [3].

388 **Proposition 4.9.** *Let μ_0 be a \mathcal{B} -eigenvalue. Take the sequence*

$$389 \quad (4.24) \quad \psi_j = \frac{H(\mu_j)g_j}{\|H(\mu_j)g_j\|_{H^{-\frac{1}{2}}(\partial D_b)}},$$

390 and (w_j, w_j^s) the associated solution of (3.7) with source term ψ_j . Then, ψ_j admits a subse-
 391 quence which converges strongly in $H^{-\frac{1}{2}}(\partial D_b)$ to $\partial_\nu w_0$, the normal trace of an eigenvector w_0
 392 of (2.5). Here, g_j is the normalised eigenvector of $\mathbf{F}(\mu_j)$ associated with $\lambda_*(\mu_j)$.

393 *Proof.* Since the sequence $(\psi_j)_j$ is bounded, it weakly converges (up to a subsequence) in
 394 $H^{-\frac{1}{2}}(\partial D_b)$ to some ψ_0 (and w_j, w_j^s converge weakly to some w_0, w_0^s in $H^1(D_b) \times H^1(B_R \setminus D_b)$).
 395 Observe that:

$$396 \quad (4.25) \quad \langle T_{\mathcal{B}}(\mu_j)\psi_j, \psi_j \rangle = \theta_j \frac{\lambda_*(\mu_j)}{|\lambda_*(\mu_j)|},$$

397 where $\theta_j := |\lambda_*(\mu_j)| / \|H(\mu_j)g_j\|_{H^{-\frac{1}{2}}(\partial D_b)}^2$ is real and $\frac{\lambda_*(\mu_j)}{|\lambda_*(\mu_j)|}$ converges to -1 by Theorem
 398 4.1. Using similar arguments as in Proposition 4.6, one can prove from equation (4.25) that
 399 $\Im m \langle T_{\mathcal{B}}(\mu_0)\psi_0, \psi_0 \rangle = 0$ and therefore w_0 satisfies (2.5). Let us show that $(\psi_j)_j$ converges
 400 strongly to ψ_0 and that ψ_0 is non trivial.

401 Using the fact that $\mu \rightarrow T_{\mathcal{B}}(\mu)$ is continuous, up to a subsequence, one can show that the
 402 sequence $(\theta_j)_j$ converges to some $\theta_0 \geq 0$. From the decomposition in Lemma 4.4, we have:

$$403 \quad (4.26) \quad \langle T_0(\mu_j)\psi_j, \psi_j \rangle = \langle T_{\mathcal{B}}(\mu_j)\psi_j, \psi_j \rangle - \langle K(\mu_j)\psi_j, \psi_j \rangle,$$

404 where $\langle T_{\mathcal{B}}(\mu_j)\psi_j, \psi_j \rangle$ converges to some negative number and $\langle K(\mu_j)\psi_j, \psi_j \rangle$ converges to
 405 $\langle K(\mu_0)\psi_0, \psi_0 \rangle$ (see proof of Proposition 4.6). We deduce that $\lim_{j \rightarrow +\infty} \langle T_0(\mu_j)\psi_j, \psi_j \rangle$ exists
 406 and that

$$407 \quad (4.27) \quad \lim_{j \rightarrow +\infty} \langle T_0(\mu_j)\psi_j, \psi_j \rangle \leq -\langle K(\mu_0)\psi_0, \psi_0 \rangle.$$

408 One can observe using the definition of $K(\mu_0)$ that $\langle K(\mu_0)\psi_0, \psi_0 \rangle = -\|w_0\|_{H^1(D_b)}^2$ and, using
 409 the coercivity of T_0 , show that

$$410 \quad (4.28) \quad \lim_{j \rightarrow +\infty} \left(\|w_j\|_{H^1(D_b)}^2 + \|w_j^s\|_{H^1(B_R \setminus D_b)}^2 \right) \leq \|w_0\|_{H^1(D_b)}^2,$$

411 which is enough to prove the strong convergence of w_j toward w_0 in $H^1(D_b)$ and the strong
 412 convergence of w_j^s in $H^1(B_R \setminus D_b)$ toward 0. Those convergences are sufficient to demonstrate
 413 that $\psi_j = \partial_\nu w_j - \partial_\nu w_j^s$ strongly converges to $\psi_0 = \partial_\nu w_0$. Since for all $j \in \mathbb{N}$, $\|\psi_j\|_{H^{-\frac{1}{2}}(\partial D_b)} = 1$,
 414 we have $\psi_0 \neq 0$. ■

415 *Remark 4.10.* In the context of imaging algorithms, the assumption $D \subset D_b$, while practi-
 416 cal for the presentation of results, is both restrictive and inappropriate, as obstacles may exist
 417 outside the region D_b . To properly formalize this scenario while maintaining the structure of
 418 the proofs, particularly to keep an eigenvalue problem within D_b , we consider the cases where
 419 D does not intersect ∂D_b (as depicted in Figure 2) and the transmission eigenvalues [11] k^2 as-
 420 sociated with D . The contribution of the obstacles $\Omega_D := D \setminus D_b$ (the component of D outside
 421 of D_b) leads to the following modifications of the operators $\mathcal{H}_{\mathcal{B}} : L^2(\mathbb{S}) \rightarrow H^{-\frac{1}{2}}(\partial D_b) \times L^2(\Omega_D)$
 422 and $T_{\mathcal{B}} : H^{-\frac{1}{2}}(\partial D_b) \times \overline{\mathcal{R}(\mathcal{H}_{\mathcal{B}})} \rightarrow H^{\frac{1}{2}}(\partial D_b) \times L^2(\Omega_D)$:

$$423 \quad (4.29) \quad \begin{cases} \mathcal{H}_{\mathcal{B}}g = (\partial_\nu u_{b,g}|_{\partial D_b}, u_{b,g}|_{\Omega_D}), \\ T_{\mathcal{B}}(\psi, u) = (w + \frac{1}{\mu}\mathcal{B}(\partial_\nu w), -k^2(1-n)(u + w^s)|_{\Omega_D}), \end{cases}$$

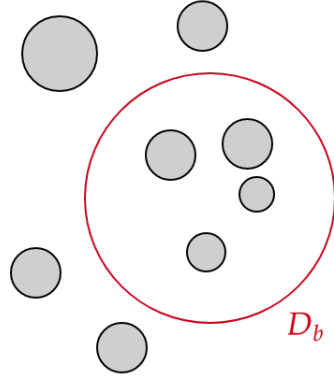


Figure 2. Example of a configuration where $D \cap \partial D_b = \emptyset$

424 where (w, w^s) are solution of:

$$425 \quad (4.30) \quad \begin{cases} \Delta w + k^2 n w = 0 \text{ in } D_b, \\ \Delta w^s + k^2 w^s = k^2 (1 - n)(u + w^s)|_{\Omega_D} \text{ in } \mathbb{R}^m \setminus D_b, \\ w^s + \frac{1}{\mu} \mathcal{B}(\partial_\nu w^s) = w + \frac{1}{\mu} \mathcal{B}(\partial_\nu w) \text{ on } \partial D_b, \\ \partial_\nu w - \partial_\nu w^s = \psi \text{ on } \partial D_b, \\ \lim_{r \rightarrow +\infty} \int_{|x|=r} \left| \frac{\partial w^s}{\partial r} - i k w^s \right|^2 = 0, \end{cases}$$

426 and $\overline{\mathcal{R}(\mathcal{H}_{\mathcal{B}})}$ denotes the closure of the range of $\mathcal{H}_{\mathcal{B}}$ in $L^2(\Omega_D)$. The decomposition in Lemma
427 4.4 still holds provided that $n > 1$ in Ω_D .

428 **5. Numerical validation of the inside-outside duality method.** The goal of this section
429 is to provide a numerical validation for the inside-outside duality method inspired by Theorem
430 4.1. Our numerical experiments will be conducted in dimension 2, meaning for $m = 2$.

431 **5.1. The case of a disc.** Consider the simple situation where $D = D_b = B_\rho$ is a disk
432 of radius $\rho > 0$ centered at the origin. We assume that n is constant inside B_ρ and $n = 1$
433 outside. For \mathcal{Q} a subset of \mathbb{N} , we use as operator \mathcal{B} in the background problem (2.2) the one
434 defined by

$$435 \quad (5.1) \quad \mathcal{B}\psi = \sum_{q \in \mathcal{Q}} \langle \psi, e_q \rangle e_q,$$

436 where $e_q(\theta) := e^{iq\theta}$, $\theta \in [0, 2\pi)$. In that case, the \mathcal{B} -eigenvalues, denoted $\mu_{\text{ref},q}$ assume the
437 following analytical expression for $q \in \mathcal{Q}$:

$$438 \quad (5.2) \quad \mu_{\text{ref},q}(n) = -2\pi k \rho \sqrt{n} \frac{J'_q(k\rho\sqrt{n})}{J_q(k\rho\sqrt{n})},$$

439 where J_j denotes the Bessel function of the first kind of order j .
 440 The far field pattern Fg due to a Herglotz wave function of the form (3.2) as an incident field
 441 with density

$$442 \quad (5.3) \quad g(\theta) = \sum_{m \in \mathbb{Z}} g_m e^{im\theta},$$

443 takes the form

$$444 \quad (5.4) \quad Fg(\theta) = \sum_{m \in \mathbb{Z}} \alpha_m g_m e^{im\theta},$$

445 where

$$446 \quad \alpha_m = i^m \sqrt{\frac{8\pi}{k}} e^{-i\frac{\pi}{4}} \frac{J'_m(k\rho)J_m(k\rho\sqrt{n}) - \sqrt{n}J_m(k\rho)J'_m(k\rho\sqrt{n})}{-J_m(k\rho\sqrt{n})H_m^1(k\rho) + \sqrt{n}J'_m(k\sqrt{n}\rho)H_m^1(k\rho)}.$$

447 Similarly, one can derive an expression of the background far field as:

$$448 \quad (5.5) \quad F_b^\mu g(\theta) = \sum_{m \in \mathbb{Z}} \beta_m g_m e^{im\theta},$$

449 where

$$450 \quad (5.6) \quad \begin{cases} \beta_m = -i^m \sqrt{\frac{8\pi}{k}} e^{-i\frac{\pi}{4}} \frac{\mu J_m(k\rho) + 2\pi\rho k J'_m(k\rho)}{\mu H_m^{(1)}(k\rho) + 2\pi\rho k H_m^{(1)'}(k\rho)}, & m \in \mathcal{Q} \\ \beta_m = -i^m \sqrt{\frac{8\pi}{k}} e^{-i\frac{\pi}{4}} \frac{J_m(k\rho)}{H_m^{(1)}(k\rho)} & \text{otherwise,} \end{cases}$$

451 We clearly observe that the eigenvalues of \mathcal{F}^μ are $(\alpha_m - \beta_m)$, $m \in \mathbb{Z}$ and they are respectively
 452 associated with the eigenvector e_m . Consequently, the eigenvalues of the scattering operator
 453 \mathbf{S} are

$$454 \quad e^{i\delta_m} := 1 + \frac{2ik}{\gamma} \left(1 - \frac{2ik}{\gamma} \overline{\beta_m}\right) (\alpha_m - \beta_m)$$

455 where $\delta_m \in [0, 2\pi)$ denote their corresponding phases. Observe that only the eigenvalues for
 456 $m \in \mathcal{Q}$ depend on μ .

457 In Figure 3 (left), we display the curves $\mu \rightarrow \delta_m(\mu)$ for $m \in \{-10, \dots, 10\}$ and $\mathcal{Q} = \{0\}$. We
 458 clearly see that the curves for $m \neq 0$ are horizontal lines, which means that they do not depend
 459 on μ . The only non constant curve $\delta_0(\mu)$ has a discontinuity at the expected \mathcal{B} -eigenvalue
 460 $\mu_{\text{ref},0}(2)$. In addition, we observe that $\delta_0(\mu) \rightarrow 2\pi$ as $\mu \rightarrow \mu_{\text{ref},0}(2)$ and $\mu > \mu_{\text{ref},0}(2)$,
 461 which coincides with Theorem 4.1. In Figure 3 (right), one can draw similar conclusions with
 462 $\mathcal{Q} = \{0, 1, 2\}$ and the presence of 3 distinct \mathcal{B} -eigenvalues.

463 **5.2. The case of other geometries using synthetic simulated data.** We consider a do-
 464 main D_b shown in Figure 4 is composed of small circular scatterers with $n = 2$ that occupy
 465 four different regions in the space (see Figure 4). The operator F cannot be computed ana-
 466 lytically in this case. It is numerically generated by solving the scattering problem (2.1) using
 467 a finite element method implemented with the FreeFEM [20] package. We use the Perfectly

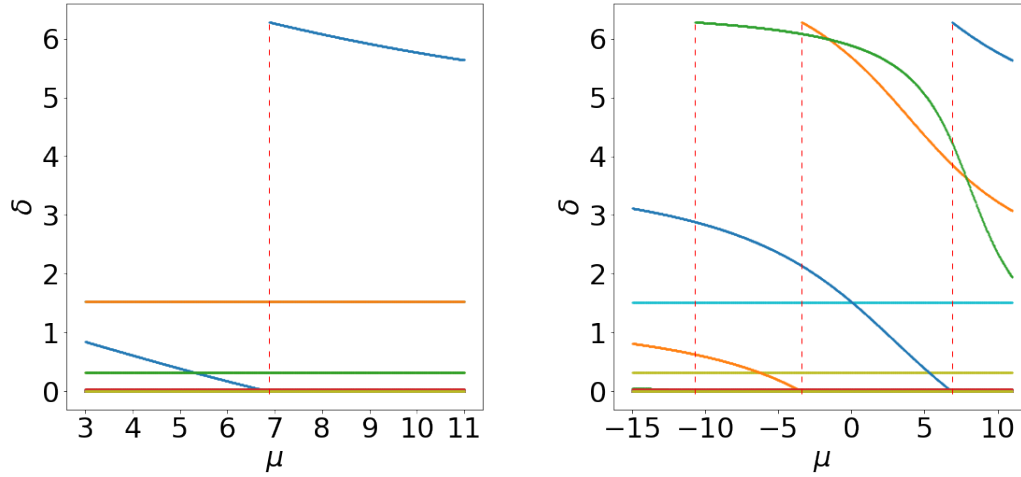


Figure 3. For $m \in \{-10, \dots, 10\}$, we plot the curves $\mu \rightarrow \delta_m(\mu)$ where $D = D_b = B_\rho$ for $\rho = 0.4333$, $k = 3$ and $n = 1$. Each color (other than red) corresponds to a value of m . The red dashed line indicates the \mathcal{B} -eigenvalue (5.2) for $\mathcal{Q} = \{0\}$ (left) and $\mathcal{Q} = \{0, 1, 2\}$ (right).

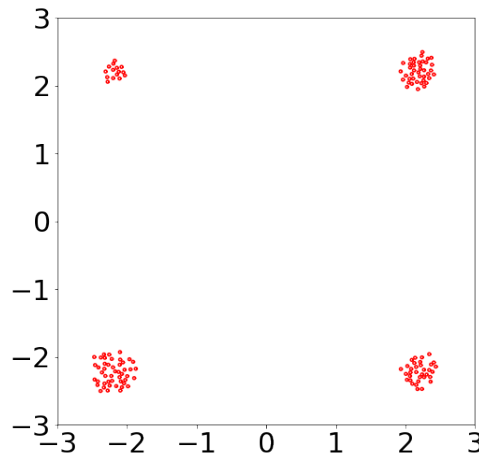


Figure 4. Left: The domain D (in red) composed of four areas in the four corners that we fill with small circular scatterers of radius 0.02 with $n = 2$ inside

468 Matched Layer ([9]) technique to bound the computational domain and model the Sommerfeld
 469 radiation condition.

470 The outcome of our numerical solver is the matrix \mathbb{F} (that plays the role of an numerical
 471 approximation of F) with entries

$$472 \quad (5.7) \quad \mathbb{F}_{pq} = u^\infty(\hat{x}_p, d_q), \quad 1 \leq p, q \leq N,$$

473 where $\hat{x}_p = d_p = (\cos(\theta_p), \sin(\theta_p))$ with $\theta_p = \frac{p}{N}2\pi$ and where u^∞ is the numerically computed
 474 far field. In this following, we take $N = 40$ and $k = 3$.

475 We shall test the inside-outside duality for the case where the domain D_b will occupy two
 476 different regions as illustrated in Figure 5 (left) and Figure 7 (left). The first one does not
 477 contain any inclusion and the second one contains one of the packs of small circles.

478
 479 Since in the following examples and in the imaging algorithm introduced later, we need to
 480 compute the background far field operator for different positions of the circular domain D_b .
 481 We therefore briefly explain how one quickly evaluates this far field operator.

482 Denote by B_ρ^y the disk of center $y \in \mathbb{R}^2$ and radius $\rho > 0$. The far field pattern $u_{b,y}^\infty$ associated
 483 with the background problem (2.2) with $D_b = B_\rho^y$ can be expressed as

$$484 \quad (5.8) \quad u_{b,y}^\infty(\hat{x}, d) = e^{iky \cdot (d - \hat{x})} u_b^\infty(\hat{x}, d),$$

485 where u_b^∞ is the far field associated with $D_b = B_\rho^0$ (i.e the disk of radius ρ centered at the
 486 origin). The far field pattern assumes the following analytic expression:

$$487 \quad (5.9) \quad u_{b,0}^\infty(\hat{x}, d) = \sum_{m \in \mathbb{Z}} \beta_m e^{im(\theta_{\hat{x}} - \theta_d)},$$

488 with $\hat{x} = (\cos(\theta_{\hat{x}}), \sin(\theta_{\hat{x}}))$, $d = (\cos(\theta_d), \sin(\theta_d))$ and β_m are given by (5.6).

489 The numerical approximation of the background far field operator $F_{b,y}^\mu$ is the background far
 490 field matrix $\mathbb{F}_{b,y}^\mu$ which entries are:

$$491 \quad (5.10) \quad (\mathbb{F}_{b,y}^\mu)_{pq} = u_{b,y}^\infty(\hat{x}_p, d_q), \quad 1 \leq p, q \leq N,$$

492 where $u_{b,y}^\infty$ is evaluated using (5.8) and where u_b^∞ is approximated by a truncation of the sum
 493 in (5.9), keeping the indices $j \in \mathbb{Z}$ such that $|j| < J$. In the following, we use $J = 10$.

494
 495 We shall illustrate how the \mathcal{B} -eigenvalues depend on the position of the domain D_b on
 496 the synthetic configuration depicted in Figure 4.

497 In Figure 5 (right), we display (for $\mathcal{Q} = \{0\}$), the curves $\mu \rightarrow \delta_m(\mu)$ associated with the
 498 configuration in Figure 5 (left) where D_b is a disk of radius $\rho = \frac{1.3}{k}$ centered at the origin with
 499 $k = 3$. Since there are no scatterers inside D_b , we expect the \mathcal{B} -eigenvalue to be equal to
 500 $\mu_{\text{ref},q}(1)$ for $q \in \mathcal{Q}$. In line with the theory, we observe that the discontinuity for one of the
 501 curves occurs at the predicted eigenvalue (represented by the red dashed line) and a behavior
 502 similar to Figure 3 (left). In the case $\mathcal{Q} = \{0, 1, 2\}$, we have the same conclusions as we obtain
 503 results represented in Figure 6 (right) that are similar to the one in Figure 3 (right). The
 504 only difference between the analytical case and this one is that the curves not associated with
 505 \mathcal{B} -eigenvalues are no longer independent from μ .

506
 507 In Figure 7 and 8, the domain D_b is the same disk as before but centered at the point
 508 (2.2, 2.2). The reference \mathcal{B} -eigenvalues cannot be analytically computed for this configuration.
 509 We numerically evaluate them by solving (2.7) using the finite element methods implemented
 510 in FreeFEM. The expression of these eigenvalues is given by (2.8). These computed values

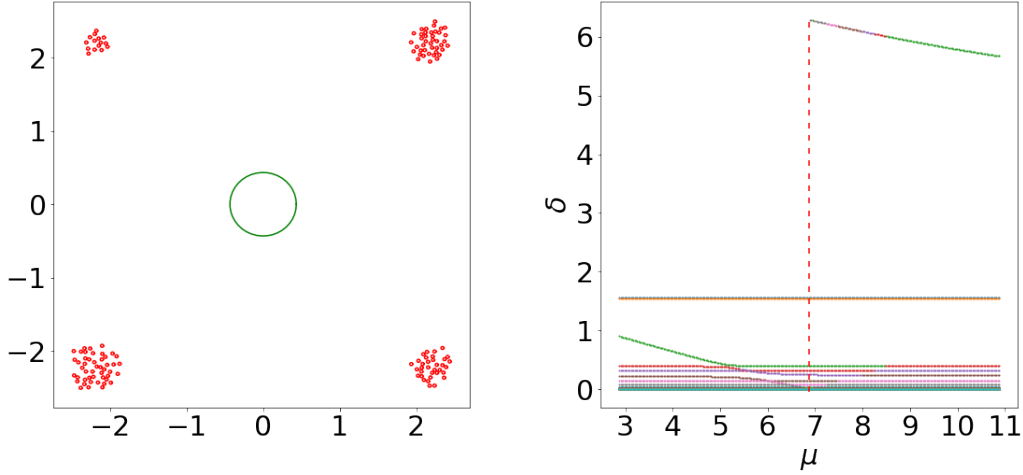


Figure 5. Left: The domain D (in red) and D_b , the disk of radius $\rho = 0.433$ (in green). Right: Plot of the curves $\mu \rightarrow \delta_m(\mu)$ for $k = 3$ and $n = 2$ inside the defects. The red dashed line indicates the analytical \mathcal{B} -eigenvalue (5.2) for constant $n = 1$ and $\mathcal{Q} = \{0\}$.

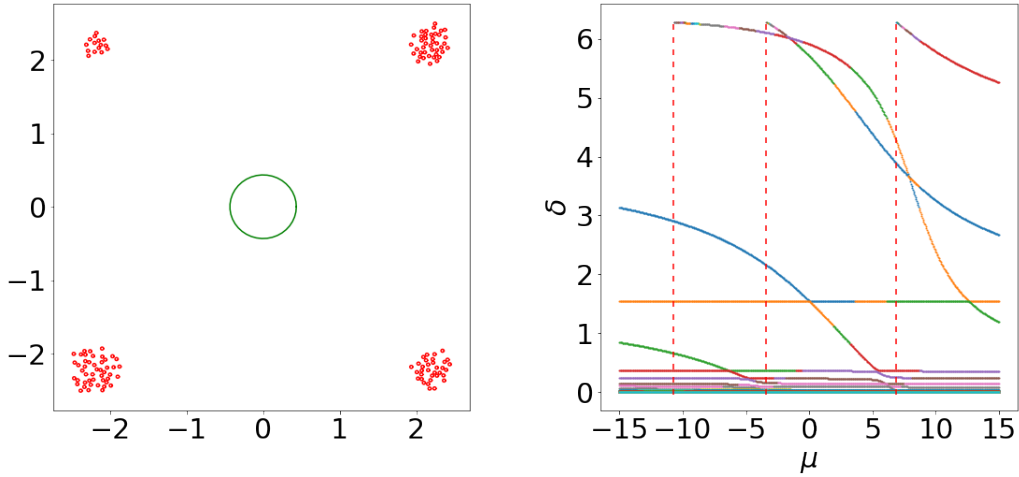


Figure 6. Left: The domain D (in red) and D_b , the disk of radius $\rho = 0.433$ (in green). Right: Plot of the curves $\mu \rightarrow \delta_m(\mu)$ for $k = 3$ and $n = 2$ inside the defects. The red dashed line indicates the analytical \mathcal{B} -eigenvalue (5.2) for constant $n = 1$ and $\mathcal{Q} = \{0, 1, 2\}$.

511 are indicated in the figures by a red straight dashed vertical line. The results for $\mathcal{Q} = \{0\}$
 512 in Figure 7 and $\mathcal{Q} = \{0, 1, 2\}$ in Figure 8 show that the inside-outside duality is capable of
 513 correctly identifying the \mathcal{B} -eigenvalues for this configuration.

514 In the imaging algorithm introduced below, we shall use $\mathcal{Q} = \{0\}$ to minimize the number
 515 of \mathcal{B} -eigenvalues that has to be determined. Figure 9 indicates the dependence of the inside-

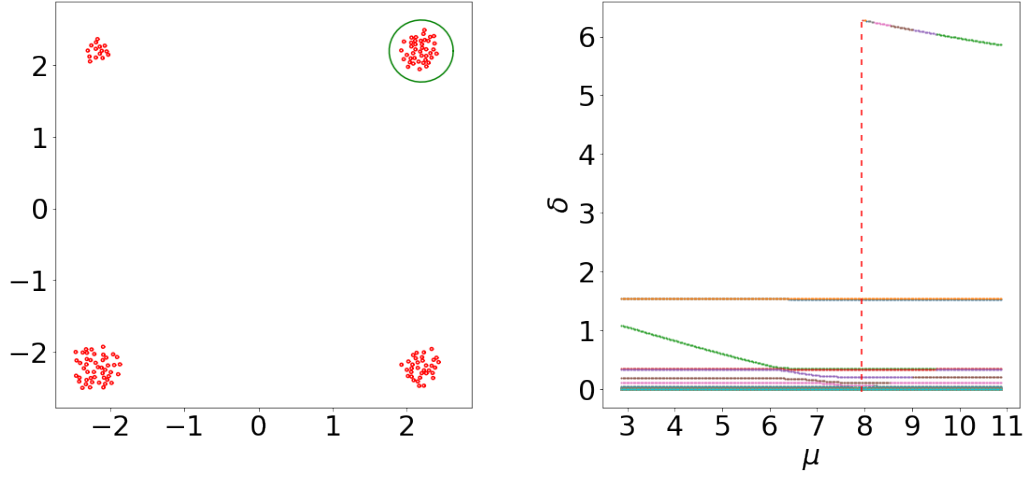


Figure 7. Left: The domain D (in red) and D_b , the ball of radius $\rho = 0.433$ centered at $(2.2, 2.2)$ (in green). Right: Plot of the curves $\mu \rightarrow \delta_m(\mu)$ for $k = 3$ and $n = 2$ inside the defects. The red dashed line indicates the approximated \mathcal{B} -eigenvalue computed with the relation (2.8) for $\mathcal{Q} = \{0\}$.

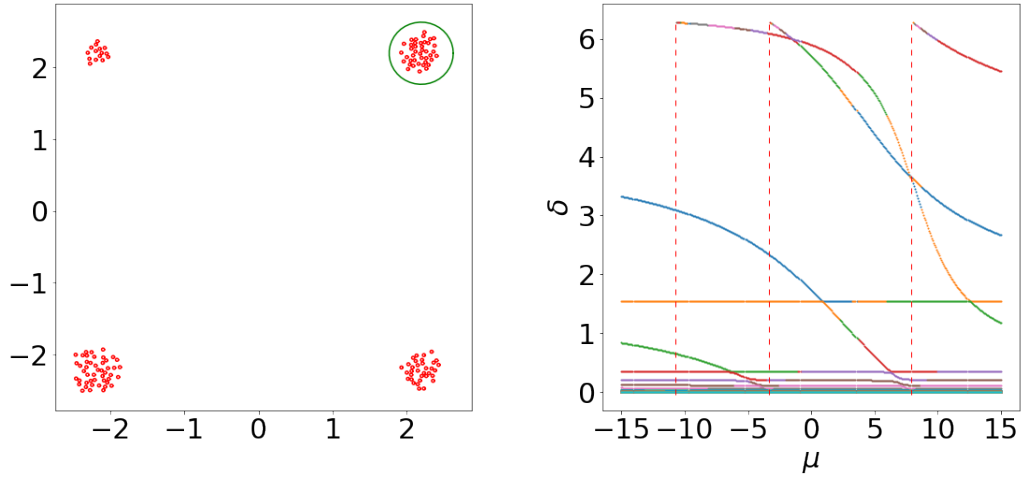


Figure 8. Left: The domain D (in red) and D_b , the ball of radius $\rho = 0.433$ centered at $(2.2, 2.2)$ (in green). Right: Plot of the curves $\mu \rightarrow \delta_m(\mu)$ for $k = 3$ and $n = 2$ inside the defects. The red dashed line indicates the approximated \mathcal{B} -eigenvalue computed with the relation (2.8) for $\mathcal{Q} = \{0, 1, 2\}$.

516 outside duality outcome with respect to noise in the data F . In order to simulate noise in
 517 the data, we change the values of the synthetic data \mathbb{F} by adding random noise of level δ to
 518 construct the noisy far field matrix $\mathbb{F}^\delta = \mathbb{F} \cdot (1 + \delta(A + iB))$ where the entries of the matrices
 519 A and B are uniformly distributed real values in $[-1, 1]$ and where \cdot denotes the element-
 520 wise product of matrices. Figure 7 clearly shows that the location of the eigenvalues is very

521 robust with respect to the noise level. This is one of the main motivations for using these
 522 \mathcal{B} -eigenvalues.

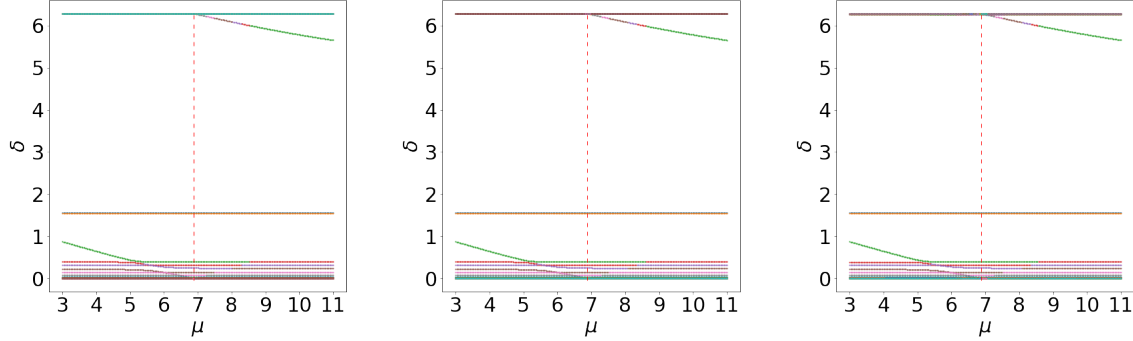


Figure 9. Plot of the curves $\mu \rightarrow \delta_m(\mu)$ for $k = 3$ and $n = 2$ inside the defects for the configuration shown in Figure 7 (left), D_b being a ball of radius $\rho = 0.4333$ centered at the origin and $\mathcal{Q} = \{0\}$ Left: $\delta = 1\%$, Middle: $\delta = 10\%$, Right: $\delta = 50\%$. The red dashed line indicates the analytical \mathcal{B} -eigenvalue (5.2) for constant $n = 1$ and $\mathcal{Q} = \{0\}$.

522

523 5.3. Application to the reconstruction of averaged values of the refractive index n .

524 Several works in the literature have proposed inversion algorithms that exploit special forms
 525 of \mathcal{B} -eigenvalues or so-called transmissions eigenvalues [8, 4, 7]. In order to determine the
 526 \mathcal{B} -eigenvalues, these contributions employ a method based on the GLSM method ([5]). We
 527 here revisit the method proposed in [7] for reconstructing the averaged values of the refractive
 528 index by replacing the GLSM with the inside-outside duality method. Let us first outline this
 529 imaging algorithm. The method uses the operator \mathcal{B} in (5.1) with $\mathcal{Q} = \{0\}$. In this case, the
 530 boundary condition on ∂D_b is of the form:

$$531 \quad (5.11) \quad \mu u + \int_{\partial D_b} \partial_\nu u ds = 0 \text{ on } \partial D_b.$$

532 In this case, there is only one \mathcal{B} -eigenvalue and the reference eigenvalue for constant index
 533 n is given by $\mu_{\text{ref},0}(n)$ in (5.2). The function $\mu_{\text{ref},0}$ is a bijection between $[0, j_0/(k\rho)[$ and \mathbb{R}^+ ,
 534 where j_0 is the first zero of J_0 .

535

The algorithm can be described with the following steps:

- 537 1. Let $\rho > 0$ be a given parameter. Choose D_b to be the ball B_ρ^y of radius ρ and center
 538 $y \in \mathcal{Y}$, a grid of points sampling the region of interest.
- 539 2. Evaluate the \mathcal{B} -eigenvalue $\mu(y, n)$ from the measurements \mathbb{F} and the analytically
 540 computed $\mathbb{F}_{b,y}^\mu$ using the inside-outside method (see *Method 1* and *Method 2* below).
- 541 3. Compute $n^*(y) \in [0, j_0/(k\rho)[$ such that $\mu(y, n) = \mu_{\text{ref},0}(n^*(y))$.
- 542 4. Plot the function $y \rightarrow n^*(y)$

543 The key step in this algorithm is (ii), that is how to automatically recover $\mu(y, n)$ from graphics
 544 as in Figure 7 (right). We indicate two possible methods.

545 *Method 1.* Let Λ be the interval of values where $\mu(y, n)$ is supposed to belong. This inter-
 546 val should contains $\mu_{\text{ref},0}(1)$. Fix a parameter small $\varepsilon > 0$ and a threshold $\sigma \in [0, 2\pi - \varepsilon)$ not
 547 too close to 0. For each μ in Λ , we compute the eigenvalues $e^{i\delta_m}$ of the operator $\mathbf{S}(\mu)$. Then
 548 we count the number of phases δ_m that belong to $[\sigma, 2\pi - \varepsilon)$. For carefully chosen ε and σ ,
 549 this number is constant for $\mu < \mu(y, n)$ in Λ and increases by 1 for the first value in Λ that
 550 exceeds $\mu(y, n)$. This allows us to identify $\mu(y, n)$.

551
 552 *Method 2.* This method exploits the observation that all the eigenvalues $e^{i\delta_m}$ slowly vary
 553 with respect to μ except one. Denote by $\hat{\delta}_m \in [-\pi, \pi)$ such that $e^{i\delta_m} = e^{i\hat{\delta}_m}$. We then ex-
 554 pect the function $\mathcal{I}(\mu) = \sum_m |\hat{\delta}_m|$ to have a minimum at $\mu(y, n)$ (see illustration in Figure 10).
 555

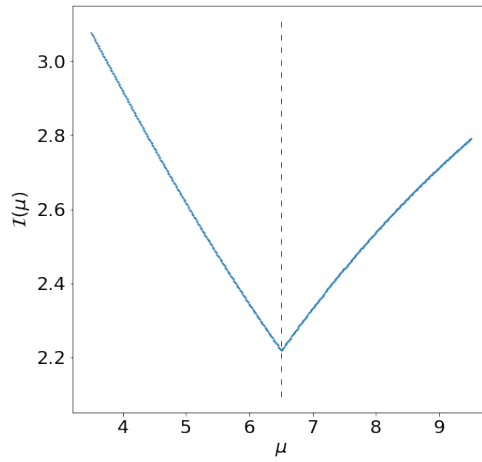


Figure 10. Plot of the curve $\mu \rightarrow \mathcal{I}(\mu)$ for $D = D_b = B_\rho$ the ball centered at the origin for $\rho = 0.3$, $k = 3$ and $n = 2$ in D . The red dashed line indicates $\mu_{\text{ref},0}(2)$.

556 In the following, we use method 1 with $\varepsilon = 10^{-2}$ and $\sigma = 2\pi - 1$. The second method
 557 also works fine and gives similar results. Before commenting the numerical tests, we briefly
 558 explain why $n^*(y)$ is expected to be an approximation of the averaged value:

559
$$\bar{n}(y) = \frac{1}{|B_\rho^y|} \int_{B_\rho^y} n(x) dx.$$

560 Consider a sequence of refractive index $(n_\varepsilon)_\varepsilon$ that converges weakly- $*$ in $L^\infty(D_b)$ to some
 561 \hat{n} as $\varepsilon \rightarrow 0$ (and denote by μ_ε its associated \mathcal{B} -eigenvalue). One can show from (2.8) that
 562 μ_ε converges to $\mu(\hat{n})$ as ε goes to 0. For highly oscillating medium, \hat{n} can be seen as an
 563 approximation of the mean value \bar{n} of n as defined above.

564 We shall test the algorithms described above for two configurations of the media as indicated
 565 in Figure 11. The configuration on the left indicates clustering of small disks with refractive
 566 index $n = 2$ and radius 0.02 with different densities in five distinct regions. The second

567 configuration on the right is formed by 4 circular inhomogeneities with different refractive
 568 index $n = 0.25$ (bottom left), $n = 0.5$ (top left), $n = 1.5$ (bottom right) and $n = 2$ (upper
 569 right). The reconstruction associated with configuration in Figure 11 (left) is shown in Figure
 570 12. In Figure 12 (left), we display the function $y \rightarrow \bar{n}(y)$ and in Figure 9 (right), we display
 571 the function $y \rightarrow n^*(y)$ resulting from the inside-outside duality with $k = 4$, $\rho = 0.33$ and
 572 the noise level $\delta = 1\%$. We clearly observe very good agreement between the two functions.
 573 Similar conclusions can be drawn from the results associated with the configuration in Figure
 574 11 (right). These results are indicated in Figure 13, where again the function $y \rightarrow \bar{n}(y)$ (left)
 575 and $y \rightarrow n^*(y)$ (right) are displayed. In this case, we used $k = 4$, $\rho = 0.3$ and the noise level
 576 $\delta = 1\%$. Observe that we chose $\rho = 0.3$ to ensure that D_b is not strictly included inside D .
 577 In fact, in this case, $\mu(y, n)$ may not be a positive value.

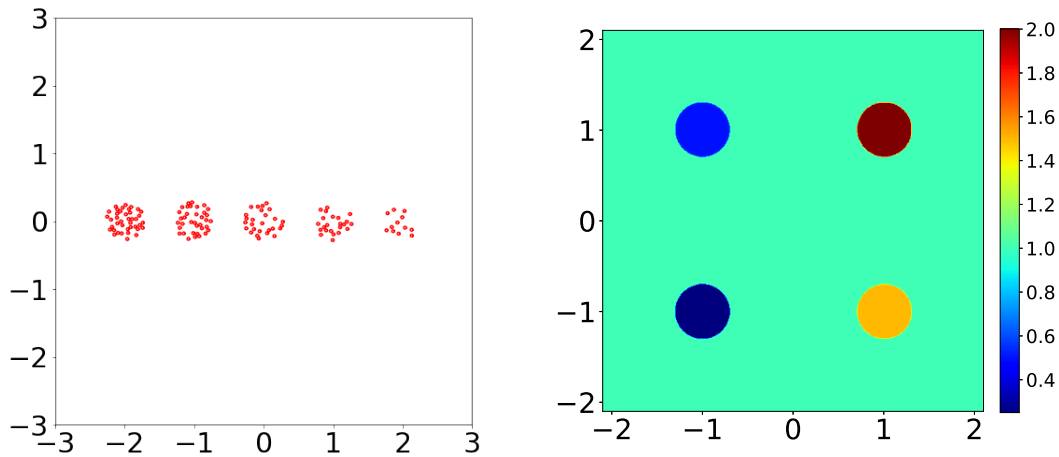


Figure 11. Left: the domain D constituted by small circles concentrated in four aligned areas. The scatterers have a radius 0.02 and a constant index refraction $n = 2$ inside. Right: Four diffracting circles of radius 0.3 associated with four different values of the refractive index $n = 0.25$ (bottom left), $n = 0.5$ (top left), $n = 1.5$ (bottom right) and $n = 2$ (upper right).

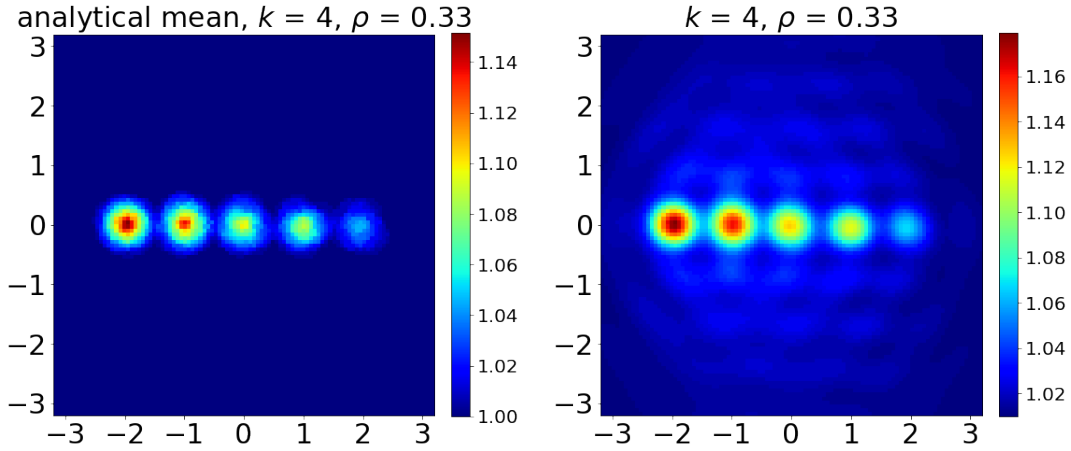


Figure 12. Results associated with configuration of the domain D in Figure 11 (left). Left: $y \rightarrow \bar{n}(y)$ representing the true averaged values of the refractive index. Right: $y \rightarrow n^*(y)$ representing the outcome of the inversion algorithm plotted on the 100×100 uniformed grid \mathcal{Y} for $k = 4$, $\rho = \frac{1.3}{k}$ and the noise level $\delta = 1\%$.

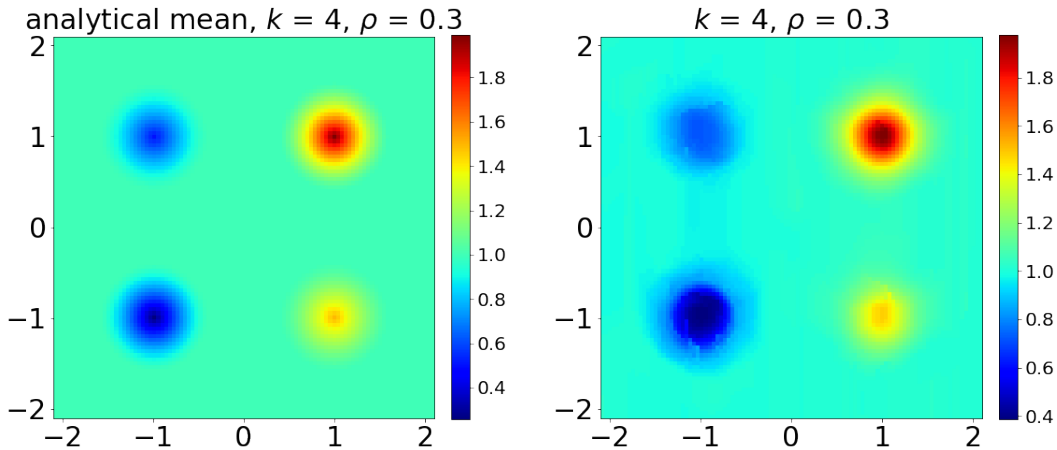


Figure 13. Results associated with configuration of the domain D in Figure 11 (right). Left: $y \rightarrow \bar{n}(y)$ representing the true averaged values of the refractive index. Right: $y \rightarrow n^*(y)$ representing the outcome of the inversion algorithm plotted on the 100×100 uniformed grid \mathcal{Y} for $k = 4$, $\rho = 0.3$ and the noise level $\delta = 1\%$.

578 **Appendix A. Structure of the \mathcal{B} operator.**

579 **Theorem A.1.** Consider a bounded linear positive, self-adjoint and compact operator $\mathcal{B} :$
 580 $H^{-\frac{1}{2}}(\partial D_b) \rightarrow H^{\frac{1}{2}}(\partial D_b)$. For κ a positive constant, the two following assertions are equivalent.

581 1. For all $\psi, \phi \in H^{-\frac{1}{2}}(\partial D_b)$,

$$582 \quad (\text{A.1}) \quad \kappa(\mathcal{B}\psi, \mathcal{B}\phi)_{L^2(\partial D_b)} = \langle \psi, \mathcal{B}\phi \rangle_{H^{-\frac{1}{2}}(\partial D_b), H^{\frac{1}{2}}(\partial D_b)}.$$

583 2. There exists a family of M vectors $\{e_1, \dots, e_M\} \subset H^{\frac{1}{2}}(\partial D_b)$ which are orthonormal
584 with respect to the $L^2(\partial D_b)$ scalar product such that:

$$585 \quad (\text{A.2}) \quad \mathcal{B}(\psi) = \kappa \sum_{i=1}^M \langle \psi, e_i \rangle_{H^{-\frac{1}{2}}(\partial D_b), H^{\frac{1}{2}}(\partial D_b)} e_i, \quad \forall \psi \in H^{-\frac{1}{2}}(\partial D_b).$$

586 *Proof.* Assume item (i) holds. Let $\mathcal{I} : H^{\frac{1}{2}}(\partial D_b) \rightarrow L^2(\partial D_b)$ denote a bijective operator.
587 Applying the spectral theorem to $\mathcal{I}\mathcal{B}\mathcal{I}^* : L^2(\partial D_b) \rightarrow L^2(\partial D_b)$, we deduce the existence of a
588 sequence of positive real number $(\lambda_i)_i$ that converges toward 0 and $(b_i)_{i \in \mathbb{N}^*}$ an orthonormal
589 basis of $L^2(\partial D_b)$ such that:

$$590 \quad \mathcal{I}\mathcal{B}\mathcal{I}^* b_i = \lambda_i b_i,$$

591 which can be rewritten as

$$592 \quad (\text{A.3}) \quad \mathcal{B}\mathcal{I}^* b_i = \lambda_i \mathcal{I}^{-1} b_i.$$

593 Every $\psi \in H^{-\frac{1}{2}}(\partial D_b)$ (respectively $\phi \in H^{\frac{1}{2}}(\partial D_b)$) admits an unique element $\tilde{\psi} \in L^2(\partial D_b)$
594 such that $\psi = \mathcal{I}^* \tilde{\psi}$ (respectively $\tilde{\phi} \in L^2(\partial D_b)$ such that $\phi = \mathcal{I}^{-1} \tilde{\phi}$).

595 Setting $a_i := (\tilde{a}, b_i)_{L^2(\partial D_b)}$, $a \in L^2(\partial D_b)$, one has:

$$596 \quad (\text{A.4}) \quad \begin{aligned} (\mathcal{B}\psi, \mathcal{B}\phi)_{L^2(\partial D_b)} &= \sum_{i,j \in \mathbb{N}^*} \phi_j \psi_i (\mathcal{B}\mathcal{I}^* b_i, \mathcal{B}\mathcal{I}^* b_j)_{L^2(\partial D_b)}, \\ &= \sum_{i,j \in \mathbb{N}^*} \phi_j \psi_i \lambda_i \lambda_j (\mathcal{I}^{-1} b_i, \mathcal{I}^{-1} b_j)_{L^2(\partial D_b)}. \end{aligned}$$

597 On the other hand:

$$598 \quad (\text{A.5}) \quad \kappa \langle \psi, \mathcal{B}\phi \rangle_{H^{-\frac{1}{2}}(\partial D_b), H^{\frac{1}{2}}(\partial D_b)} = \kappa \sum_{i \in \mathbb{N}^*} \phi_i \psi_i \lambda_i.$$

599 Since (A.4) and (A.5) should be equal for every square summable sequences $(\phi_i)_i, (\psi_i)_i$, taking
600 $\phi_k \psi_l = \delta_{ik} \delta_{li}$, we obtain that λ_i is equal to 0 or $\kappa \|\mathcal{I}^{-1} b_i\|_{L^2(\partial D_b)}^{-2}$. Since \mathcal{I} is bounded, the
601 sequence $(\|\mathcal{I}^{-1} b_i\|^2)_i$ remains also bounded. We deduce by compactness of the operator \mathcal{B}
602 that (up to a renumbering) the sequence $(\lambda_i)_i$ is equal to $\kappa \|e_i\|_{L^2(\partial D_b)}^{-2}$ up to a certain rank M
603 $\lambda_i = 0$ for $i > M$.

604 For $k, l \leq M$, setting $\phi_k \psi_l = \delta_{ik} \delta_{lj}$ enforces $(\mathcal{I}^{-1} b_k, \mathcal{I}^{-1} b_l)_{L^2(\partial D_b)} = 0$ for $k \neq l$ and $k, l \leq M$.

605 Hence, for all $\psi \in H^{-\frac{1}{2}}(\partial D_b)$, the operator \mathcal{B} can be written as:

$$606 \quad (\text{A.6}) \quad \begin{aligned} \mathcal{B}\psi &= \mathcal{B}\mathcal{I}^* \mathcal{I}^{*-1} \psi \\ &= \kappa \sum_{i=0}^M (\mathcal{I}^{*-1} \psi, b_i)_{L^2(\partial D_b)} \mathcal{I}^{-1} b_i \\ &= \kappa \sum_{i=0}^M \langle \psi, e_i \rangle_{H^{-\frac{1}{2}}(\partial D_b), H^{\frac{1}{2}}(\partial D_b)} e_i, \end{aligned}$$

607 where $e_i = \frac{\mathcal{I}^{-1} b_i}{\|\mathcal{I}^{-1} b_i\|_{L^2(\partial D_b)}}$. This proves that (i) implies (ii). The reciprocal is straightforward. ■

608 **Appendix B. Study of the background problem (2.2).** The well posedness of problem
 609 (2.2) is established by variational approach. Let B_R be a ball containing D_b for R large enough.
 610 We define the Dirichlet to Neumann map $\Lambda : H^{\frac{1}{2}}(\partial B_R) \rightarrow H^{-\frac{1}{2}}(\partial B_R)$ by $\Lambda\phi := \partial_\nu v|_{\partial B_R}$,
 611 where v is the radiating solution to the Helmholtz equation in $\mathbb{R}^m \setminus B_R$ with $v = \phi$ on ∂B_R ,
 612 and where ν is the outward unit normal to S_R . Define the closed subspace of $H^1(B_R \setminus D_b)$:

$$613 \quad (B.1) \quad H_B^1(B_R \setminus D_b) := \{w \in H^1(B_R \setminus D_b), w|_{\partial D_b} \in \mathcal{B}(H^{-\frac{1}{2}}(\partial D_b))\}.$$

614 Then, by Green's formula and using property (2.4), one can prove that solving the scatter-
 615 ing problem (2.2) is equivalent to solving the following variational problem: $u \in H_B^1(B_R \setminus D_b)$,
 616

$$617 \quad (B.2) \quad \int_{B_R \setminus D_b} (\nabla u \nabla v - k^2 uv) dx - \int_{\partial B_R} \Lambda uv ds - \mu \kappa \int_{\partial D_b} uv ds = \ell(v)$$

618 for all $v \in H_B^1(B_R \setminus D_b)$, where

$$619 \quad (B.3) \quad \ell(v) := \int_{\partial B_R} (\partial_\nu u^i - \Lambda u^i) v ds,$$

620 The study of the well-posedness of this problem follows classical schemes based on proving
 621 that the problem is of Fredholm type and the uniqueness is a consequence of Rellich's lemma.
 622 The details are left to the reader. We then can state the following lemma.

623 **Lemma B.1.** *Problem (B.2) is well posed for $\mu \in \mathbb{R}^*$ if $(\partial_\nu u^i - \Lambda u^i) \in H^{-\frac{1}{2}}(\partial B_R)$.*

624 We prove in the following lemma the normality of the operator F_b^μ .

625 **Proposition B.2.** *For $\mu \in \mathbb{R}^*$, F_b^μ is normal and $S_b = I + \frac{2ik}{\bar{\gamma}} F_b^\mu$ is unitary.*

626 *Proof.* This proof is similar to the one in [21, Theorem 1.8].

627 We first show that for all $g, h \in L^2(\mathbb{S})$,

$$628 \quad (B.4) \quad 2ik(F_b^\mu g, F_b^\mu h)_{L^2(\mathbb{S})} = \gamma(F_b^\mu g, h)_{L^2(\mathbb{S})} - \bar{\gamma}(g, F_b^\mu h)_{L^2(\mathbb{S})}.$$

629 Let us deal with the three terms independently.

630 1. Let w_g^s and w_h^s radiating solution of problem (2.2) with u^i an Herglotz wave of kernel
 631 g and h respectively with far field pattern w_g^∞, w_h^∞ . We denote by w_g^t, w_h^t the total
 632 fields. Let B_R be a disk of radius $R > 0$ centered at the origin containing D_b . Applying
 633 Green second theorem, we get

$$634 \quad 0 = \int_{\partial B_R} (\partial_\nu w_g^s \overline{w_h^s} - \partial_\nu \overline{w_h^s} w_g^s) ds - \int_{\partial D_b} (\partial_\nu w_g^s \overline{w_h^s} - \partial_\nu \overline{w_h^s} w_g^s) ds.$$

635 Letting $R \rightarrow +\infty$ and using the radiation condition, one obtains

$$636 \quad 2ik(F_b^\mu g, F_b^\mu h)_{L^2(\mathbb{S})} = 2ik \int_{\mathbb{S}} w_g^\infty \overline{w_h^\infty} ds = \int_{\partial D_b} (\partial_\nu w_g^s \overline{w_h^s} - \partial_\nu \overline{w_h^s} w_g^s) ds.$$

637 2. If $u^i = v_h$ an Herglotz wave of kernel $h \in L^2(\mathbb{S})$, then we have

$$\begin{aligned}
 \int_{\partial D_b} (\partial_\nu w_g^s \overline{v_h} - \partial_\nu \overline{v_h} w_g^s) ds &= \int_{\mathbb{S}} \overline{h}(d) \int_{\partial D_b} (\partial_\nu w_g^s e^{-iky \cdot d} - \partial_\nu e^{-iky \cdot d} w_g^s ds(y)) ds(d) \\
 &= -\gamma \int_{\mathbb{S}} w_g^\infty(d) \overline{h}(d) ds(d) \\
 &= -\gamma (F_b^\mu g, h)_{L^2(\mathbb{S})}.
 \end{aligned}$$

638

639 Similarly, one gets

$$\int_{\partial D_b} (\partial_\nu v_g \overline{w_h^s} - \partial_\nu \overline{w_h^s} v_g) ds = \overline{\gamma} (g, F_b^\mu h)_{L^2(\mathbb{S})}$$

640

641 3. We then compute $-2ik(F_b g, F_b h) + \gamma(F_b g, h) - \overline{\gamma}(g, F_b h)$:

$$\begin{aligned}
 &= -2ik \int_{\mathbb{S}} w_g^\infty \overline{w_h^\infty} ds + \gamma \int_{\mathbb{S}} w_g^\infty(d) \overline{h}(d) ds(d) - \overline{\gamma} \int_{\mathbb{S}} \overline{w_h^\infty}(d) g(d) ds(d) \\
 &= \int_{\partial D_b} (w_g^t(y) \partial_{\nu(y)} \overline{w_h^t}(y) - \overline{w_h^t}(y) \partial_{\nu(y)} w_g^t(y)) ds(y) \\
 &= -\frac{1}{\mu} \int_{\partial D_b} (\mathcal{B}(\partial_{\nu(y)} w_g^t(y)) \partial_{\nu(y)} \overline{w_h^t}(y) + \frac{1}{\mu} \mathcal{B}(\partial_{\nu(y)} \overline{w_h^t}(y)) \partial_{\nu(y)} w_g^t(y)) ds(y) \\
 &= (\frac{1}{\mu} - \frac{1}{\mu}) \int_{\partial D_b} (\mathcal{B}(\partial_{\nu(y)} w_g^t(y)) \partial_{\nu(y)} \overline{w_h^t}(y)) ds(y) \\
 &= 0,
 \end{aligned}$$

642

643 because $\mu \in \mathbb{R}$.

644 Therefore, one has:

$$(B.5) \quad F_b^{\mu*} F_b^\mu = \frac{1}{2ik} (\gamma F_b^\mu - \overline{\gamma} F_b^{\mu*}).$$

645

646 From this equality, one can easily show that $S_b^* S_b = I$ and, because S_b is a compact pertur-
 647 bation of I , conclude that S_b is unitary. This is enough to prove that F_b^μ is normal. ■

648

REFERENCES

- 649 [1] T. ARENS, R. GRIESMAIER, AND R. ZHANG, *Monotonicity-based shape reconstruction for an inverse*
 650 *scattering problem in a waveguide*, Inverse Problems, 39 (2023), p. 075009, [https://doi.org/10.1088/](https://doi.org/10.1088/1361-6420/acd4e0)
 651 [1361-6420/acd4e0](https://doi.org/10.1088/1361-6420/acd4e0), <https://dx.doi.org/10.1088/1361-6420/acd4e0>.
 652 [2] L. AUDIBERT, L. CHESNEL, AND H. HADDAR, *Transmission eigenvalues with artificial background for ex-*
 653 *PLICIT material index identification*, Comptes Rendus Mathematique, 356 (2018), pp. 626–631, [https://](https://doi.org/https://doi.org/10.1016/j.crma.2018.04.015)
 654 doi.org/https://doi.org/10.1016/j.crma.2018.04.015, [https://www.sciencedirect.com/science/article/](https://www.sciencedirect.com/science/article/pii/S1631073X18301298)
 655 [pii/S1631073X18301298](https://www.sciencedirect.com/science/article/pii/S1631073X18301298).
 656 [3] L. AUDIBERT, L. CHESNEL, AND H. HADDAR, *Inside-outside duality with artificial backgrounds*, Inverse
 657 Problems, 35 (2019), p. 104008, <https://hal.science/hal-02095660>.
 658 [4] L. AUDIBERT, L. CHESNEL, H. HADDAR, AND K. NAPAL, *Qualitative indicator functions for imaging*
 659 *crack networks using acoustic waves*, 2020, <https://arxiv.org/abs/2006.10342>.
 660 [5] L. AUDIBERT AND H. HADDAR, *A generalized formulation of the Linear Sampling Method with exact*
 661 *characterization of targets in terms of farfield measurements*, Inverse Problems, 30 (2014), [https://](https://doi.org/10.1088/0266-5611/30/3/035011)
 662 doi.org/10.1088/0266-5611/30/3/035011, <https://inria.hal.science/hal-00911692>.
 663 [6] L. AUDIBERT AND H. HADDAR, *A generalized formulation of the linear sampling method with exact*
 664 *characterization of targets in terms of farfield measurements*, Inverse Problems, 30 (2014), p. 035011.

- 665 [7] L. AUDIBERT, H. HADDAR, AND F. POURRE, *Imaging highly heterogeneous media using transmission*
666 *eigenvalues*, in 2023 IEEE Conference on Antenna Measurements and Applications (CAMA), 2023,
667 pp. 597–600, <https://doi.org/10.1109/CAMA57522.2023.10352698>.
- 668 [8] L. AUDIBERT, H. HADDAR, AND F. POURRE, *Reconstruction of averaging indicators for highly hetero-*
669 *geneous media*, *Inverse Problems*, 40 (2024), p. 045028, <https://doi.org/10.1088/1361-6420/ad2f64>,
670 <https://dx.doi.org/10.1088/1361-6420/ad2f64>.
- 671 [9] E. BÉCACHE, S. FAUQUEUX, AND P. JOLY, *Stability of perfectly matched layers, group velocities and*
672 *anisotropic waves.*, *Journal of Computational Physics*, 188 (2003), pp. 399–433, [https://doi.org/10.](https://doi.org/10.1016/S0021-9991(03)00184-0)
673 [1016/S0021-9991\(03\)00184-0](https://doi.org/10.1016/S0021-9991(03)00184-0), <https://ensta-paris.hal.science/hal-00989051>.
- 674 [10] F. CAKONI, D. COLTON, AND H. HADDAR, *On the determination of dirichlet or transmission eigen-*
675 *values from far field data*, *Comptes Rendus Mathématique*, 348 (2010), pp. 379–383, [https://doi.](https://doi.org/https://doi.org/10.1016/j.crma.2010.02.003)
676 [org/https://doi.org/10.1016/j.crma.2010.02.003](https://doi.org/https://doi.org/10.1016/j.crma.2010.02.003), [https://www.sciencedirect.com/science/article/pii/](https://www.sciencedirect.com/science/article/pii/S1631073X10000476)
677 [S1631073X10000476](https://www.sciencedirect.com/science/article/pii/S1631073X10000476).
- 678 [11] F. CAKONI, D. COLTON, AND H. HADDAR, *Inverse Scattering Theory and Transmission Eigenvalues*,
679 vol. 98, CBMS-NSF, Dec. 2022.
- 680 [12] S. COGAR, *A modified transmission eigenvalue problem for scattering by a partially coated crack*, *Inverse*
681 *Problems*, 34 (2018), p. 115003.
- 682 [13] S. COGAR, D. COLTON, S. MENG, AND P. MONK, *Modified transmission eigenvalues in inverse scattering*
683 *theory*, *Inverse Problems*, 33 (2017), p. 125002.
- 684 [14] D. COLTON, F. CAKONI, AND P. MONK, *Nondestructive testing and target identification*, (2016).
- 685 [15] D. COLTON AND A. KIRSCH, *A simple method for solving inverse scattering problems in the resonance*
686 *region*, *Inverse Problems*, 12 (1996), pp. 383–393.
- 687 [16] D. COLTON AND R. KRESS, *Inverse Acoustic and Electromagnetic Scattering Theory*, Applied Mathemat-
688 ical Sciences, Springer Berlin Heidelberg, 2013, <https://books.google.fr/books?id=U5wemvIDnNwC>.
- 689 [17] J. ECKMANN AND C. PILLET, *Spectral duality for planar billiards*, *Comm. Math. Phys.*, 170 (1995),
690 pp. 283–313.
- 691 [18] R. GRIESMAIER AND B. HARRACH, *Monotonicity in inverse medium scattering on unbounded domains*,
692 *SIAM Journal on Applied Mathematics*, 78 (2018), pp. 2533–2557.
- 693 [19] H. HADDAR, M. KHENISSI, AND M. MANSOURI, *Inside-Outside Duality for Modified Transmission Eigen-*
694 *values*, *Inverse Problems and Imaging*, 17 (2022), pp. 798–816, <https://doi.org/10.3934/ipi.2023004>,
695 <https://inria.hal.science/hal-03876859>.
- 696 [20] F. HECHT, *New development in freefem++*, *Journal of Numerical Mathematics*, 20 (2012), [https://doi.](https://doi.org/10.1515/jnum-2012-0013)
697 [org/10.1515/jnum-2012-0013](https://doi.org/10.1515/jnum-2012-0013).
- 698 [21] A. KIRSCH AND N. GRINBERG, *The Factorization Method for Inverse Problems*, Oxford Univer-
699 sity Press, 12 2007, <https://doi.org/10.1093/acprof:oso/9780199213535.001.0001>, [https://doi.org/10.](https://doi.org/10.1093/acprof:oso/9780199213535.001.0001)
700 [1093/acprof:oso/9780199213535.001.0001](https://doi.org/10.1093/acprof:oso/9780199213535.001.0001).
- 701 [22] A. KIRSCH AND A. LECHLEITER, *The inside–outside duality for scattering problems by inhomogeneous*
702 *media*, *Inverse Problems*, 29 (2013), p. 104011, <https://doi.org/10.1088/0266-5611/29/10/104011>.
- 703 [23] A. LECHLEITER AND S. PETERS, *The inside–outside duality for inverse scattering problems with near field*
704 *data*, *Inverse Problems*, 31 (2015), p. 085004.